The Binding of Concanavalin a to the Surface of Intact and Denuded Sea Urchin Eggs Affects the Fertilization Process by Altering the Structural Dynamics of Actin Filaments

Nunzia Limatola *, Marinella Pirozzi, Davide Caramiello, Jong Tai Chun, Luigia Santella *

Posted Date: 3 June 2025

doi: 10.20944/preprints202506.0164.v1

Keywords: acrosome reaction; sea urchin eggs; jelly coat; species-specificity recognition; bindin; vitel-line layer; Concanavalin A, fertilization; actin; calcium

 doi:10.20944/preprints202506.0164.v1

Article

The Binding of Concanavalin a to the Surface of Intact and Denuded Sea Urchin Eggs Affects the Fertilization Process by Altering the Structural Dynamics of Actin Filaments

Nunzia Limatola [1,4], Marinella Pirozzi [2], Davide Caramiello [3], Jong Tai Chun [4] and Luigia Santella [1,*]

[1] Department of Research Infrastructures for Marine Biological Resources, Stazione Zoologica Anton Dohrn, 80121 Napoli, Italy; nunzia.limatola@szn.it; santella@szn.it

[2] Institute of Endotypes in Oncology, Metabolism, and Immunology "G. Salvatore," National Council of Research (IEOMI-CNR), Via Pietro Castellino 111, Naples, Italy; marinella.pirozzi@ieos.cnr.it

[3] Department of Marine Animal Conservation and Public Engagement, Stazione Zoologica Anton Dohrn, 80121 Napoli, Italy; davide.caramiello@szn.it

[4] Department of Biology and Evolution of Marine Organisms, Stazione Zoologica Anton Dohrn, 80121 Napoli, Italy; chun@szn.it

* Correspondence: N.L nunzia.limatola@szn.it; L.S. santella@szn.it

Abstract: In *Paracentrotus lividus* eggs, we assessed the binding capacity of the lectin Concanavalin A to the glycoproteins present in the vitelline layer, which is tightly bound to the membrane of the microvilli on the sea urchin egg's surface. We aimed to understand the role of carbohydrate residues in species-specific gamete recognition and binding. This interaction occurs after the sperm undergoes the jelly coat-induced acrosome reaction, which exposes the adhesive protein bindin, allowing the fusion of sperm and egg membranes, ultimately leading to fertilization. Our findings reveal that, while fertilization of both intact and denuded eggs (from which the jelly coat and vitelline layer were removed) in the presence the lectin does not affect sperm functionality, it influences the Ca^{2+} response of the activated egg and the penetration of sperm in a dose-dependent manner. Comparative analyses of the effect of Concanavalin A on the fertilization response, assessed through light, fluorescence, confocal, and electron microscopy, revealed significant alterations in the structural dynamics of the actin filaments on the surface and cortex of the eggs responsible for the altered Ca^{2+} signals. In addition to the visualization of the binding of the lectin with the vitelline layer of intact eggs and membranes of denuded eggs, the usage of a fluorescently tagged lectin has also enabled, for the first time, the visualization of the glycoprotein contents of the outer jelly coat.

Keywords: acrosome reaction; sea urchin eggs; jelly coat; species-specificity recognition; bindin; vitelline layer; Concanavalin A; fertilization; actin; calcium

1. Introduction

For more than a hundred years, sea urchins have served as an excellent experimental model for studying fertilization in vitro since their gametes can be obtained in large quantities and easily manipulated and observed in the Petri dish containing seawater, i.e., in experimental conditions closely resembling what happens at sea. However, despite the enormous knowledge and insights gained from this fundamental process, our understanding of the fertilization of this marine organism is not yet complete and remains a work in progress. The reports in the literature describe a generalized scheme of fertilization-associated reactions, including sperm activation and the acquisition of motility triggered by seawater, which increases intracellular pH and the respiration

 doi:10.20944/preprints202506.0164.v1

rate, as well as by egg-derived sperm-activating peptides that induce Ca^{2+}-dependent sperm chemotaxis [1]. It has also been shown that the components of the egg jelly (jelly coat, JC) surrounding sea urchin eggs trigger the acrosome reaction (AR) in vitro, during which the acrosomal vesicle in the anterior portion of the sperm head undergoes exocytosis, allowing the species-specificity binding of the fertilizing sperm with the egg membrane [2–8]. Since the JC preparations of some sea urchin species induced the AR in homologous sperm, it was suggested that the specific induction of the AR was due to the structural uniqueness of the JC in the pattern of sulfation and the glycosidic linkage of the polysaccharides [1,9]. The AR leads to the extension of the acrosomal process (AP) following actin polymerization, which exposes bindin at the tip of the sperm head. This adhesive protein interacts with the sperm receptors on the thin vitelline layer (VL) of the egg, which tightly adheres to the microvilli (MV) containing actin emerging from the egg membrane by "vitelline posts" [10–13]. Further proteolytic treatments of the unfertilized eggs with enzymes showed that the broken-up of the VL on the egg surface reduced the fertilizability of eggs by disrupting the sperm-binding site on the VL [14]. Additional studies showed that during the cortical reaction of the fertilized egg, some proteases are released from the cortical granules (CG) undergoing exocytosis and deposited into the perivitelline space (PS), thereby breaking the linkages between the VL and the plasma membrane of the MV. The action of proteases at the time of the separation of the VL from the egg plasma membrane also alters the sperm receptor sites. It facilitates the detachment of supernumerary sperm (slow block to polyspermy) [15–17]. In line with this, trypsin inhibitors, which block the elevation of the fertilization envelope (FE) and sperm detachment, lead to polyspermy, which is detrimental to normal development [16,18,19]. Incorporating structural proteins deriving from the extruded CG contents induces the structuralization of the PS and the subsequent hardening of the elevating VL to form the FE, which protects the embryo [20–22]. Following fertilization, it was also possible to analyze the nature of the proteins from CG after their exocytosis in seawater from eggs where the VL had been previously disrupted by dithiothreitol (DTT) [23]. The subsequent events of the fertilization process involving the penetration of the VL by the AP of the activated sperm and fusion between the egg membranes of sperm and egg have been poorly understood due to the rapidity of the process and to the fact that only one of the multiple sperm attached to the VL will fuse with the egg plasma membrane and penetrate it [19,24–26].

According to the prevailing view, the exposed bindin on the sperm AP is essential for the sperm to recognize and bind to its receptors of the egg VL [27]. However, the fertilization response of *P. lividus* eggs has been shown to occur even when the JC and VL have been structurally altered or removed from unfertilized eggs [26,28–31], indicating that these layers are not essential for the activation of sperm. In sea urchin eggs, the fertilization process is characterized by an initial phase involving the depolarization of the egg plasma membrane, which coincides with F-actin-linked Ca^{2+} signals a few seconds after the fusion of the sperm and egg membranes [32–34]. These events strictly depend on the morphology of MV containing actin filaments and the structural integrity of cortical granules/vesicles associated with the egg plasma membrane, which is crucial for the proper changes that occur during egg activation [35–38]. The sperm-induced Ca^{2+} increase before and during the exocytosis of the CG coincides with the visible depolymerization of the F-actin in the outer region of the cytoplasm (ectoplasm) of the egg. During the egg's contraction, it forms a dimple, which reflects the initial separation of the VL from the egg plasma membrane [39–42]. This early Ca^{2+}-dependent cortical reaction is a prerequisite for the subsequent metabolic activation and embryonic development phase. During this late fertilization phase, starting 5 minutes after insemination, the development of K^+ conductance, MV elongation, and cortical actin polymerization induced by an intracellular pH increase [19,43–48] counteract the c F-actin-linked depolymerization of the egg surface taking place a few seconds after sperm addition [31,42]. The cortical actin remodeling at the site of sperm-egg binding involves the formation of a cone of actin filaments (fertilization cone, FC) to engulf the sperm first visualized at the transmission electron microscope in sea urchin eggs preincubated and inseminated in the presence of nicotine to induce polyspermy and thereby to increase the chances of cutting ultrathin sections through the multiple FC [49,50]. It is important to

 doi:10.20944/preprints202506.0164.v1

note that recent studies have shown that nicotine treatment of *P. lividus* eggs induces polyspermic entry by dramatically altering the dynamics of the egg's F-actin, leading to abnormal sperm penetration in the activated eggs [51].

Previous studies on the interactions of the fertilizing sperm with the surface of sea urchin eggs also aimed at understanding the role of the glycoprotein components of the sperm receptors in the VL. The results showed that the lectin Concanavalin A (Con A), which can precipitate with numerous polysaccharides [52], can prevent fertilization at a concentration higher than 0.1 mg/ml in several sea urchin species [53–55]. Insight into the nature of the effect of Con A on sea urchin fertilization and incubation of intact *Strongilocentrotus purpuratus* eggs with fluorescent Con A revealed its high affinity binding to the VL sites but not the JC. The removal or alteration of the VL by dithiothreitol [23] reduces the number of Con A binding sites on the plasma membrane (low affinity) of unfertilized eggs [55]. Following fertilization of eggs deprived of the VL, the increased number of Con A binding sites on the egg plasma membrane was suggested to be due to the insertion of the membranes of the CG following their exocytosis [54,56]. These results indicated that the interaction of Con A with the "naked" plasma membrane of *S. purpuratus* eggs did not prevent the attachment and fusion of the sperm with the egg and the induction of the cortical reaction [54,55]. Subsequently, the great variety of conflicting observations about the effect of Con A on the fertilization process of different sea urchin eggs was argued to be due to the crosslinking of the specific carbohydrate residues of the sperm receptors with which the Con A binds, let alone how the fertilization was conducted [57].

In the present investigation, to resolve the contradictory results in the literature on the role of the VL glycoprotein in the species-specificity gamete interaction, we exposed *P. lividus* eggs to different concentrations of Con A and studied their effect on the morpho-functional aspects of the fertilization process. Upon insemination, the initiation of the sperm-induced Ca^{2+} signal representing the sperm-egg fusion has been employed as criteria with which to judge whether the binding of Con A with the VL carbohydrate residues could affect sperm-egg interaction and egg activation. Our electron microscopy examinations have revealed that 5 minutes of exposure of intact and denuded *P. lividus* to Con A significantly alters the topography of the egg surface, e.g., the ultrastructure of the VL, microvilli, and cortical granules. These egg surface morphological changes induced by lectin incubation do not prevent the interaction and fusion of the sperm with the egg plasma membrane, nor do they delay the onset of the first sperm-induced Ca^{2+} signal at the periphery of the egg (cortical flash, CF), but heavily affect the pattern of the Ca^{2+} response at fertilization. Our use of standard fluorescence and confocal microscopy, along with a fluorescent version of Con A, to investigate the interaction of Con A with the VL of intact eggs and the plasma membrane of denuded eggs has enabled the first visualization of lectin binding to the outer JC.

2. Materials and Methods

2.1. Gamete Preparation and Fertilization

Sea urchins (*Paracentrotus lividus*) were collected in the Gulf of Naples from December to April and kept in a tank with circulating seawater at 16 °C. Spawning was induced by intracoelomic injection of 0.5 M KCl into female and male animals. Eggs were collected in natural seawater (NSW) filtered with a Millipore membrane (pore size 0.2 µm, Nalgene vacuum filtration system, Thermo Fisher Scientific, Rochester, NY, USA) and used for the experiments within 3 hours after spawning. Denuded eggs were prepared by incubating intact unfertilized eggs for 20 min in NSW containing 10 mM DTT at pH 9.0 and adjusted with NaOH [26,30] to remove the extracellular coat (the outer egg jelly and vitelline layer). For insemination of the eggs, the dry sperm collected from male animals were diluted in NSW only a few minutes before fertilization at the final concentration of 1.84×10^6 cells/mL.

 doi:10.20944/preprints202506.0164.v1

2.2. Time-lapse movies of the fertilization process and visualization of the sperm in intact and denuded eggs

The fertilization response (cortical structural and Ca^{2+} changes) of intact and denuded eggs with and without Concanavalin A (Con A) treatment was monitored by epifluorescence microscopy with a cooled CCD (charge-coupled device) camera (CoolSNAP HQ^2 camera, Photometrics) mounted on a Zeiss Axiovert 200 inverted microscope (Carl Zeiss AG, Oberkochen, Germany) with a Plan-Neofluar 40×/0.75 and 20x/0.5 objectives and a CMOS camera (CoolSNAP Myo, Photometrics) mounted on a Zeiss Axiovert 135 TV with a Plan-Neofluar 40x/0.75 objective and a XBO 75 W lamp. Diluted sperm in NSW were stained with 5 µM of the nuclear dye Hoechst-33342 (Sigma-Aldrich, St. Louis, MO, USA) for 30 s before fertilization. The visualization of the decondensed DNA of the male pronucleus detected the number of fluorescent sperm incorporated into fertilized eggs.

2.3. Scanning Electron Microscopy (SEM)

Intact and denuded *P. lividus* eggs exposed to Concanavalin A (Con A) were fixed before and after insemination in NSW containing 0.5% glutaraldehyde (pH 8.1) for 1 h at room temperature and post-fixed with 1% osmium tetroxide for another hour. After several rinses, the specimens were dehydrated in ethanol with increasing concentrations and then subjected to critical point drying using a LEICA EM CP300. The samples were coated with a thin layer of gold using a LEICA ACE200 sputter coater and were observed with a JEOL 6700F scanning electron microscope (Akishima, Tokyo, Japan).

2.4. Transmission Electron Microscopy (TEM)

Intact and denuded eggs treated in the same experimental conditions described for SEM observations were fixed directly in NSW containing 0.5% glutaraldehyde (pH 8.1) for 1 h at room temperature. They were post-fixed with 1% osmium tetroxide and 0.8% $K_3Fe(CN)_6$ for another hour at 4 °C. After washing three times in NSW, the samples were rinsed twice in distilled water for 10 min and subsequently treated with 0.15% tannic acid for 1 min at room temperature. After extensive rinsing in distilled water (10 min, three times), the samples were dehydrated in acetone with increasing concentrations and transferred to a solution made of acetone and SPURR before being embedded in SPURR. Resin blocks were sectioned with a Leica EM UC7 ultramicrotome, and the ultrathin sections (70 nm in thickness) were observed with FEI TECNAI G2 Spirit BioTWIN 120 kV Transmission Electron Microscope (FEI Company, Eindhoven, Netherlands) equipped with a Veleta CCD digital camera (Olympus Soft Imaging Solutions GmmbH, Münster, Germany).

2.5. Chemicals, Reagents, and Recombinant Proteins

Concanavalin A (Con A) and the fluorescent Con A (Alexa Fluor 633) were purchased from Sigma Aldrich and Invitrogen (Molecular probes, Inc. Eugene, OR, USA) and dissolved in distilled water and 0.1 M Sodium bicarbonate, respectively. Unless specified otherwise, all reagents used in this study were purchased from Sigma Aldrich. The recombinant protein LifeAct-GFP was bacterially expressed [30,31,42,58] from the plasmid kindly provided by Dr. A. McDougall of Sorbonne University, France. BPA-C8-Cy3 was synthesized and generously provided by Dr. J-M Lehn and his colleagues, following the chemical procedure that was described in detail elsewhere [29].

2.6. Microinjection, Ca^{2+} Imaging, Fluorescence and Confocal Microscopy

Freshly spawned intact eggs were microinjected with an air pressure transjector (Eppendorf FemtoJet, Hamburg, Germany), as previously described [29,34]. To detect the sperm-induced intracellular Ca^{2+} increase, 500 µM Calcium Green 488 conjugated with 10 kDa dextran was mixed with 35 µM Rhodamine Red (Molecular Probes, Eugene, OR, USA) in the injection buffer (10 mM Hepes, 0.1 M potassium aspartate, pH 7.0) and microinjected into the eggs before insemination. The relative fluorescence signals of the cytosolic Ca^{2+} were acquired with a cooled CCD camera (CoolSNAP HQ2, Photometrics) mounted on a Zeiss Axiovert 200 microscope with a Plan-Neofluar

 doi:10.20944/preprints202506.0164.v1

20x/0.5 to simultaneously monitor the sperm-induced Ca^{2+} signals in several eggs (average of n=6) and a CMOS camera (CoolSNAP Myo, Photometrics) mounted on a Zeiss Axiovert 135 TV with a Plan-Neofluar 40x/0.75 objective at about 3 s intervals. The data were analyzed with MetaMorph (Universal Imaging Corporation, Molecular Devices, LLC, San Jose, CA, USA). Following the formula $F_{rel} = [F - F_0]/F_0$, where F represents the average fluorescence level of the entire egg, and F_0 is the baseline fluorescence, the overall Ca^{2+} signals were quantified for each moment. F_{rel} was expressed as RFU (relative fluorescence unit) for plotting the Ca^{2+} trajectories.

2.7. Visualization of Actin Filaments in the Egg Cortex

LifeAct-GFP (10 μg/μL, pipette concentration) was microinjected into live intact eggs to visualize the cortical F-actin. To visualize the binding of the fluorescent Concanavalin A (Con A), eggs were exposed to Alexa Fluor 633 Con A (Invitrogen, Molecular Probes) With or without removing the vitelline layer (VL). Before and after fertilization, the intact and denuded eggs treated with the fluorescent lectin were observed with a Leica TCS SP8X confocal laser scanning microscope equipped with a white light laser and hybrid detectors (Leica Microsystem, Wetzlar, Germany), using different pinholes as described in the Results section.

2.8. Statistical Analysis

The numerical MetaMorph data were compiled and analyzed with Excel (Microsoft Office 2010) and reported as mean ± standard deviation in all cases in this manuscript. One-way ANOVA was performed through Prism 5.0 (GraphPad Software), and $p < 0.05$ was considered statistically significant. Results showing $p < 0.05$ indicated the statistical significance of the difference between the two groups, which was assessed using Tukey's post hoc tests.

3. Results

3.1. Effect of Concanavalin A exposure on the fertilization envelope elevation and sperm entry

Unfertilized *P. lividus* eggs were treated with different concentrations of Concanavalin A (Con A) in seawater or for 5 minutes (see the histograms in Figure 1) and subsequently inseminated in the presence or absence (after washing) of the lectin. To monitor the progress of fertilization, the elevation of the FE was examined, and the number of egg-incorporated sperm was counted by use of the vital fluorescent dye Hoechst 33342 that prestained the sperm DNA.

Figure 1 shows the bright field image (upper panel) of the FE being elevated in intact eggs 5 minutes after insemination (control). In the panels below, the epifluorescence microscopic images show a single sperm (arrow), which fused with the female pronucleus (arrowhead). Con A treatment at a concentration of 1 mg/ml for 5 minutes completely inhibits the formation of the FE, which could not be reversed by washing off Con A with NSW before insemination (data not shown) in line with the previous reports for *P. lividus* and other sea urchin species [53,57]. Exposure of the eggs at this concentration of Con A before insemination also blocks sperm entry in all the examined eggs (Table 1 and Figure 1).

 doi:10.20944/preprints202506.0164.v1

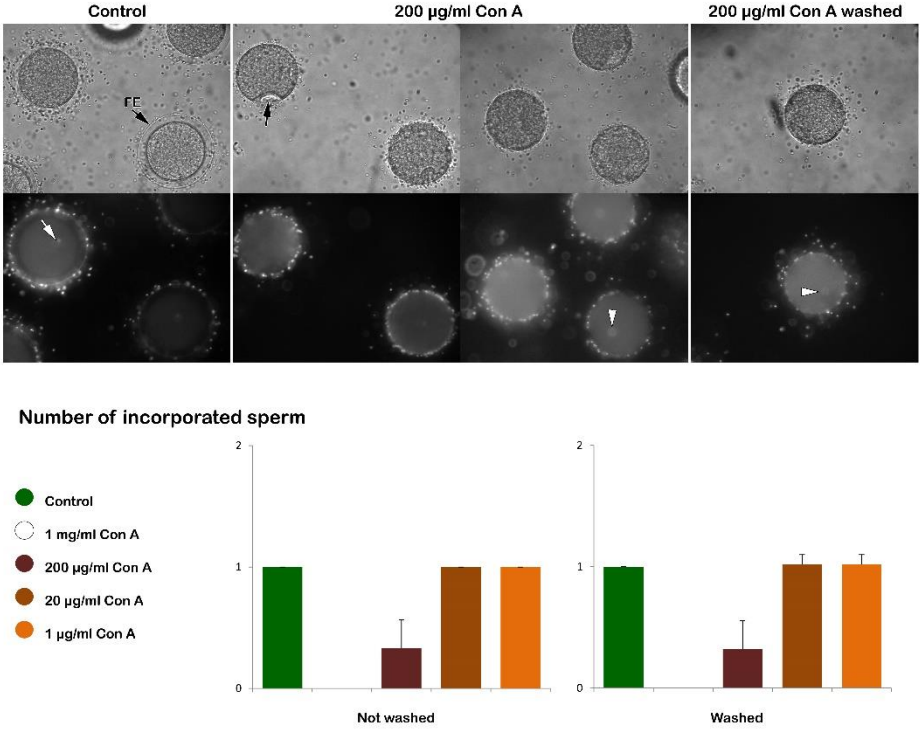

Figure 1. Effect of Concanavalin A (Con A) on fertilization. Intact *P. lividus* was pretreated with Con A for 5 min before insemination. The bright field image in the upper panel illustrates the progressive elevation of the fertilization envelope (FE) being blocked in the eggs fertilized after Con A treatment. A noticeable dimple (arrow) on the egg surface fails to lead to elevated FE but remains visible even 5 minutes after insemination. The representative epifluorescence images show the fertilizing sperm stained with Hoechst-33342 in the control eggs 5 minutes post-insemination (arrow). The exposure to Con A (> 200 µg/ml) inhibited sperm entry, regardless of whether the eggs were washed; only the female pronucleus is visible in the epifluorescence image (arrowhead).

Table 1. Number of egg-incorporated sperm with various concentrations of Con A in the medium.

Sperm entry	0	1 mg/ml Con A	200 µg/ml Con A	20 µg/ml Con A	1 µg/ml Con A
Mean ± SD	1 ± 0	0 ± 0*	0.33 ± 0.23*	1 ± 0	1 ± 0
n	60	60	60	60	60

* $P < 0.01$.

Whereas the 5-minute pretreatment with 1 mg/ml Con A consistently prevented the *P. lividus* eggs from being fertilized, the same pretreatment with a lower dose of Con A (200 µg/ml) displayed a more subtle effect. As shown in the bright field image of Figure 1, eggs pretreated with Con A and inseminated with or without washing the lectin formed a prominent concavity (dimple, arrow) on the egg surface beneath the separated vitelline layer (VL), which reflects contraction of the cortical cytoskeletal elements. While this cytoplasmic change is temporary in the control eggs at fertilization, this dimple remained 5 minutes after insemination. Nonetheless, the epifluorescence image of the same egg showed that the fertilizing sperm entered the egg and fused with the female pronucleus (arrow). At variance with control eggs, the dimple formation occurs about 10-15 seconds after insemination at the initiation of the separation of the VL from the egg surface and concomitant with the depolymerization of the cortical F-actin and cortical granules (CG) exocytosis [25,26,42]. Such cortical deformation detected at the light microscopical level in several sea urchin species [39,40] is transient as the eggs resume their spherical shape concomitantly with the FE elevation over the entire egg surface, as shown in the control of Figure 1.

 doi:10.20944/preprints202506.0164.v1

Table 2. Number of egg-incorporated sperm with various concentrations of Con A after washing.

Sperm Entry	0	1 mg/ml Con A WASHED	200 µg/ml Con A WASHED	20 µg/ml Con A WASHED	1 µg/ml Con A WASHED
Mean ± SD	1 ± 0	0 ± 0*	0.32 ± 0.23*	1.02 ± 0.08	1.02 ± 0.08
n	40	40	40	40	40

* P < 0.01.

Our previous studies showed that the removal of the egg jelly (jelly coat, JC) and VL promoted polyspermic fertilization [26,30], demonstrating that the specific interaction and fusion of numerous sperm with the egg does occur at the level of the egg plasma membrane and not VL [59]. We now examine the effect of Con A on the fertilization response of denuded eggs. Figure 2 shows the incorporation of numerous sperm after fertilizing *P. lividus* eggs pretreated with 10 mM of DTT at pH 9 for 20 min to remove the associated VL and JC. The absence of the JC is evident in the two neighboring denuded eggs that came in close vicinity due to the lack of the extracellular layers that would otherwise expel other eggs, as shown in the light microscopy image in A (upper panel). The number of supernumerary sperm entering the eggs (Table 3) was counted 5 minutes after insemination are shown in the lower panel in (arrows) and histograms of Figure 2. When denuded eggs were treated with Con A (200 µg/ml) and inseminated, the fertilized eggs failed to incorporate sperm in most cases, as the only DNA signal came from the female pronucleus (arrowhead) in the cytoplasm. In other cases, the denuded eggs pretreated with Con A were penetrated by only one sperm, thus reducing the polyspermic fertilization rat (Figure 2 B, lower panel and histograms).

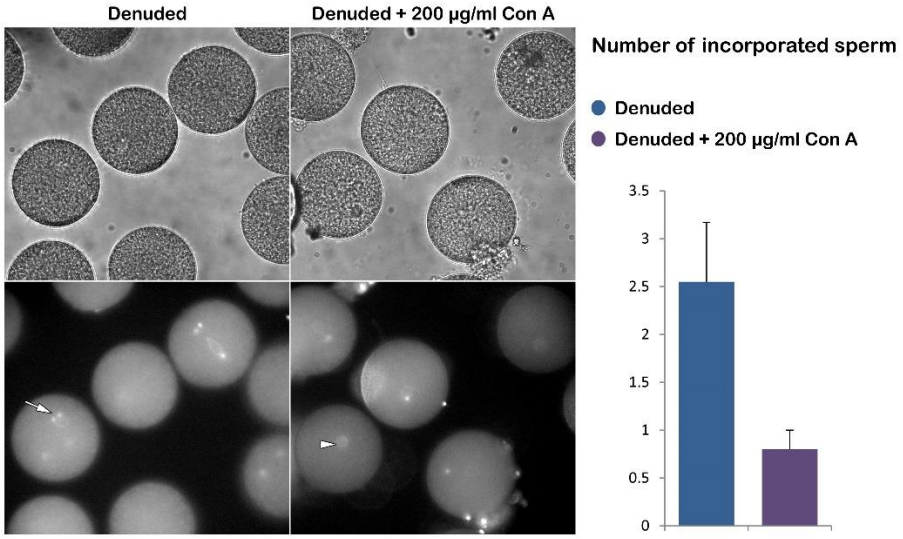

Figure 2. Effect of Con A on fertilization of denuded *P. lividus* eggs. The bright field image in the upper panel shows that the vitelline layer did not separate to form the FE due to its prior removal from the unfertilized eggs. As a result, a noticeable dimple did not form on the egg surface, indicating the impact of Con A on fertilization-induced egg contraction. The representative epifluorescence images display multiple sperm stained with Hoechst-33342 in the denuded eggs 5 minutes post-insemination (arrow) and the female pronucleus (arrowhead). This tendency of polyspermy is alleviated by the pretreatment of the denuded eggs with Con A, as shown in the histograms.

Table 3. Number of egg-incorporated sperm in denuded eggs with or without Con A.

Sperm Entry	Denuded	Denuded + 200 µg/ml Con A
Mean ± SD	2.55 ± 0.62	0.8 ± 0.2*
N	60	60

* P< 0.01.

 doi:10.20944/preprints202506.0164.v1

We then used Alexa Fluor 633 Concanavalin A (Fluor Con A) to visualize the glycoprotein components of the VL and the plasma membrane of intact and denuded eggs. We monitored their modifications following fertilization (Figure 3). The fluorescent lectin signals were localized only on the VL of intact eggs when the confocal microscope was set to a pinhole of diameter of 1.0 Airy Units (AU) to block out-of-focus light during image formation. At this default setting, it is only possible to detect the fluorescence of the lectin on the VL tightly attached to the egg plasma membrane and not the peripheral JC (n=12). However, examination of the samples under the confocal microscope using a pinhole aperture (hole) at a bigger size (4 AU instead of 1) allowed the production of brighter images representing the JC associated with the VL. The fluorescent Con A labeling of the JC and VL (n=12 intact) was also detected by epifluorescence microscopy using the CCD camera for the sperm-induced Ca^{2+} imaging, as shown in Supplementary Figure 1. It is noteworthy that the fluorescent Con A labels the plasma membrane of unfertilized eggs (n= 15) from which the VL and JC have been removed (Figure 3). Due to the absence of the VL, this weaker fluorescence is attributed to the low-affinity binding of the lectin to the egg plasma membrane, which has been reported in the previous studies on other sea urchin species [54].

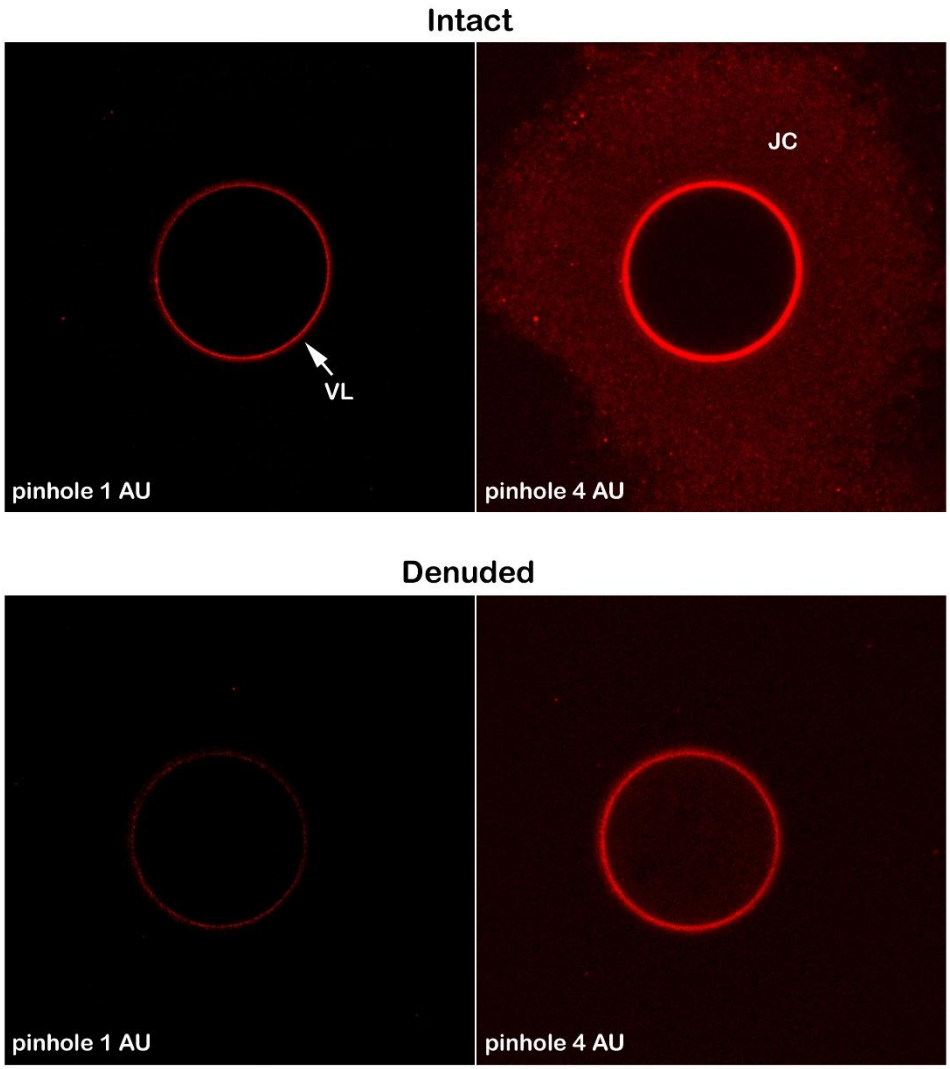

Figure 3. Fluorescent Concanavalin A binding on the extracellular matrix (jelly coat, JC and vitelline layer, VL) of intact unfertilized eggs and the membrane of denuded eggs. The peripheral JC of intact eggs was disclosed with Alexa Fluor 633 Con A by using a pinhole setting at 4 AU. On the other hand, the lectin tightly binding to the VL was visualized using a pinhole setting of 1 AU (arrow). A low-affinity lectin binding to the egg membrane was observed using the 1 AU pinhole setting when comparing intact eggs to denuded eggs lacking VL (see also Supplementary Figure S1).

 doi:10.20944/preprints202506.0164.v1

3.2. Effect of Concanavalin A exposure on the surface of intact sea urchin eggs before and after fertilization visualized with electron microscopy (scanning and transmission)

Examination of the surface topography of intact unfertilized *P. lividus* eggs using scanning electron microscopy (SEM) has confirmed our previously published results on the disappearance of the JC adhering to the VL during the fixation process, a well known fact [25,26, As a result, SEM image of the fixed *P. lividus* eggs exhibits regularly spaced microvilli (MV) containing F-actin protruding from the egg surface and tightly covered by the indistinguishable VL (Figure 4 A). After fertilization, VL detaches itself from the egg plasma membrane to form the FE (Figure 4 B), which is aided by exocytosis of the cortical granules (CG) at the egg plasma membrane. Indeed, transmission electron microscopy (TEM) of ultrathin sections shows better the thin VL covering microvilli beneath the egg plasma membrane; CG with different content morphology are also evident (Figure 4 C). Five minutes after insemination, CG became scarce in the cortical region of the activated eggs due to exocytosis of their content into the perivitelline space (PS), an event they undergo during the cortical fertilization reaction lasting about 1 minute to lead to the elevation of the FE over the entire egg surface (Figure 4 D). The TEM micrograph in Figure 4 D also shows MV elongated in the PS, as well as the formation of the hyaline layer (HL) resulting from CG exocytosis. The separated VL, in the meantime, transformed into FE, which appeared thicker than VL in TEM.

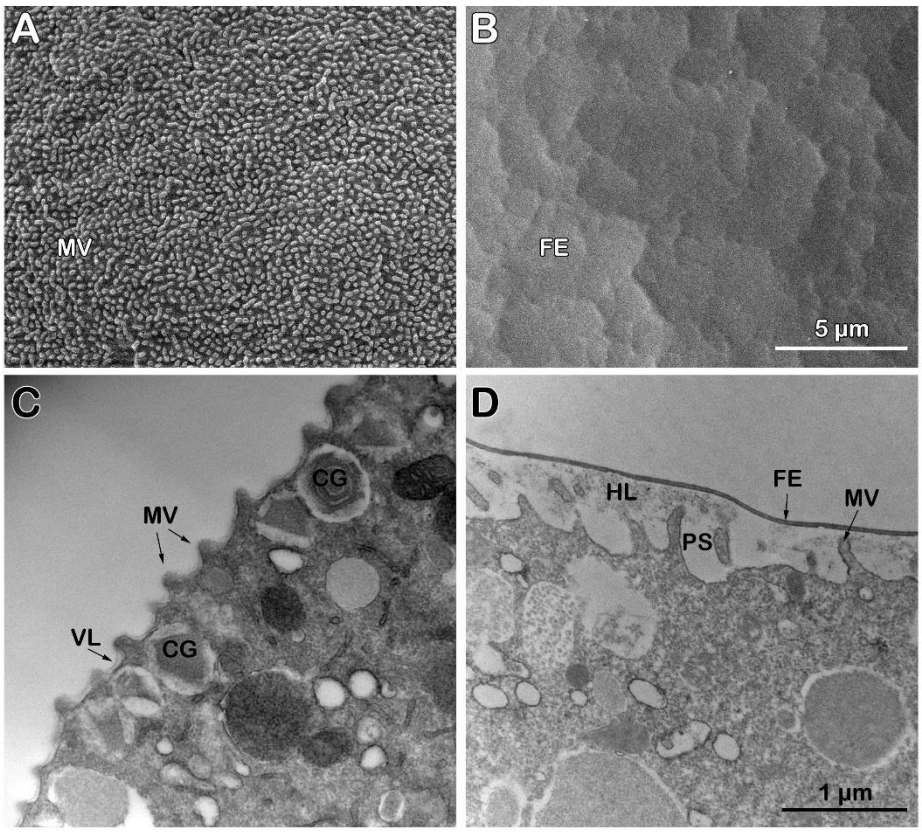

Figure 4. Scanning and transmission electron micrographs of the intact *P. lividus* eggs before and after fertilization. (**A**) A scanning electron micrograph shows microvilli (MV) regularly distributed on the surface of an unfertilized egg. (**B**) Five minutes post-insemination, FE forms and elevates over the surface of the activated egg. (**C**) A transmission electron micrograph reveals the surface of an unfertilized egg with MV covered by the vitelline layer (VL), along with secretory cortical granules (CG) located beneath the egg's plasma membrane. (**D**) Five minutes after insemination, elongated MV amid the hyaline layer (HL) fill the perivitelline space (PS) beneath the FE.

 doi:10.20944/preprints202506.0164.v1

The exposure of the intact eggs to Con A (200 µg/ml) induces slight shrinkage of the egg surface, as shown in the SEM micrograph (Figure 5 A). The effect of the lectin in altering the structural dynamics of the egg surface is markedly evident in the intact eggs pretreated with Con A for 5 minutes before insemination. An evident microvillar structural alteration by the lectin results in the inhibition of the separation and thickening of the VL from the egg plasma membrane, which usually occurs for VL to transform into the FE (Figs. 4 B and D). In line with an alteration of the VL structure, Figure 5 B shows MV projections still attached to the internal face of the FE 5 minutes after insemination compared to the fully elevated FE in control shown in Figure 4 B. The fortuitous rupture of the impaired FE structure, which fails to detach from MV in eggs treated with Con A and then inseminated, shows an inhomogeneous and irregular MV elongation in the PS interspersed with surface areas lacking MV (Figure 5 C). The inhibited separation of the VL from the egg plasma membrane due to the alteration of its structure induced by Con A treatment [57] is also evident at the ultrastructural level. The TEM micrograph of Figure 5 D shows the effect of the lectin on the morphology of the unfertilized egg surface and cortical cytoplasm. At variance with the control (Figure 4 C), the TEM image of the Con A-pretreated eggs (5 min) showed what is underneath the mildly shrunk surface and how the cortical region is changed: i) irregularity of the MV morphology, ii) CG being located deeper in the egg cytoplasm (Figure 5 D). At fertilization, the detachment of a thin FE from the egg plasma membrane is inhibited in these eggs (Figure 5 E). Moreover, their cortex still retained intact CG that failed to fuse with the egg membrane to release their content into the PS, thus preventing the thickening of the FE and the propagation of the cortical reaction along the entire egg surface (see Figure 4 for a comparison with the control).

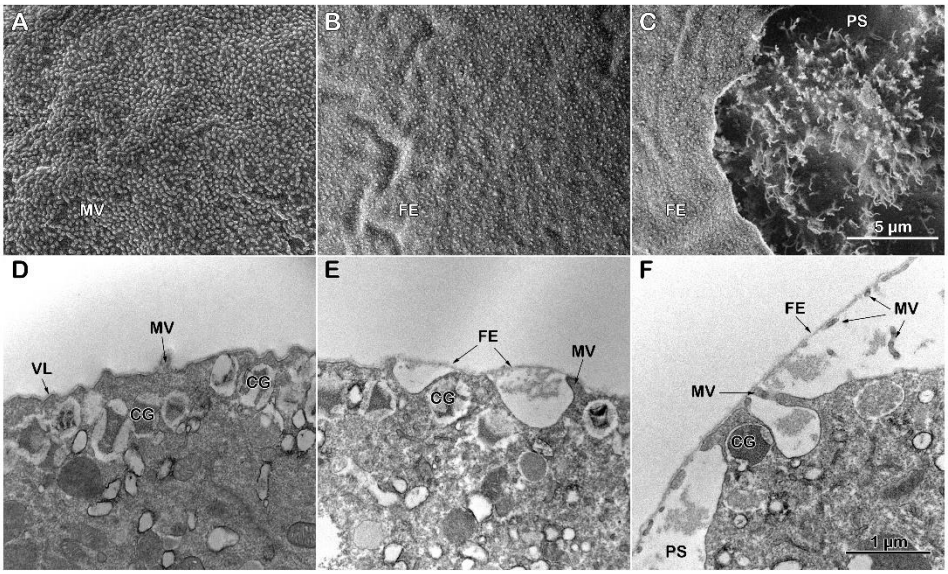

Figure 5. Scanning and transmission electron micrographs of the fertilization response of intact *P. lividus* eggs pretreated with Con A before insemination. (**A**) A scanning electron micrograph displays microvilli (MV) distributed on the surface of an unfertilized egg exposed to Con A for 5 minutes before fertilization. (**B**) Five minutes after insemination, the FE does not elevate on the surface. (**C**) In the perivitelline space (PS) of the fertilized eggs, MV elongation is observed where the FE attached to the MV's tips was ruptured. (**D**) A transmission electron micrograph shows the surface of an unfertilized egg exposed to Con A, highlighting altered MV morphology and secretory cortical granules (CG) located deeper within the egg's cytoplasm. (**E**) Five minutes after insemination, the induction and propagation of CG exocytosis are inhibited in Con A-pretreated eggs, as evidenced by isolated events of the CG exocytosis, which lead to the separation of the vitelline layer precursor of the FE. (**F**) Bound to Con A, the VL of the intact eggs fails to detach itself from the MV of the egg membrane at the time of fertilization. Note that, compared to the control shown in Figure 4 D, the FE is thinner due to the incomplete exocytosis of the CG.

 doi:10.20944/preprints202506.0164.v1

The SEM micrograph of Figure 6 A visually attests to the morphological changes on the surface of an unfertilized *P. lividus* egg from which the VL and the JC associated with it had been previously stripped off (denuded). As we previously reported [26,30], the removal of the VL, which tightly adheres to the MV, drastically alters the MV morphology and reduces its number on the egg surface, presumably decreasing the cytoskeletal retraction within the MV. Insemination of the denuded eggs in NSW promotes the entry of more than one sperm, as shown by the three fertilization cones (FC) on the egg surface of Figure 6 B and C. As expected, the activation of denuded eggs by sperm occurs without the elevation of the FE due to the absence of the VL, the precursor of the FE [26,30]. A closer examination of the SEM micrograph revealed a non-uniform MV elongation at the site of sperm fusion (Figure 6 C) to form the fertilization cones due to the reorganization of the F-actin within and around the MV, as was previously reported [29]). Indeed, MV on the egg surface are interspersed with holes, presumably through which the CG have released their contents after fusing with the egg plasma membrane directly into the seawater [16–19]. The ultrastructure of the surface of a denuded egg before fertilization (Figure 6 D) confirms the SEM observations of a reduced number of MV on the egg surface and the lack of the VL, in comparison with the intact eggs shown in Figure 4 C [26,30]. At fertilization, the separation of the VL from the egg plasma membrane and its subsequent thickening due to the apposed material secreted by the CG into the PS to form the FE is inhibited for the stripping of the VL from the plasma membrane of the unfertilized eggs (Figure 6E). Although non-uniformly, MV elongation on the fertilized egg surface still occurs in areas where they are present. The hyaline layer (HL) was retained during the fixation amid the elongated MV in the absence of the FE elevation (Figure 6 E).

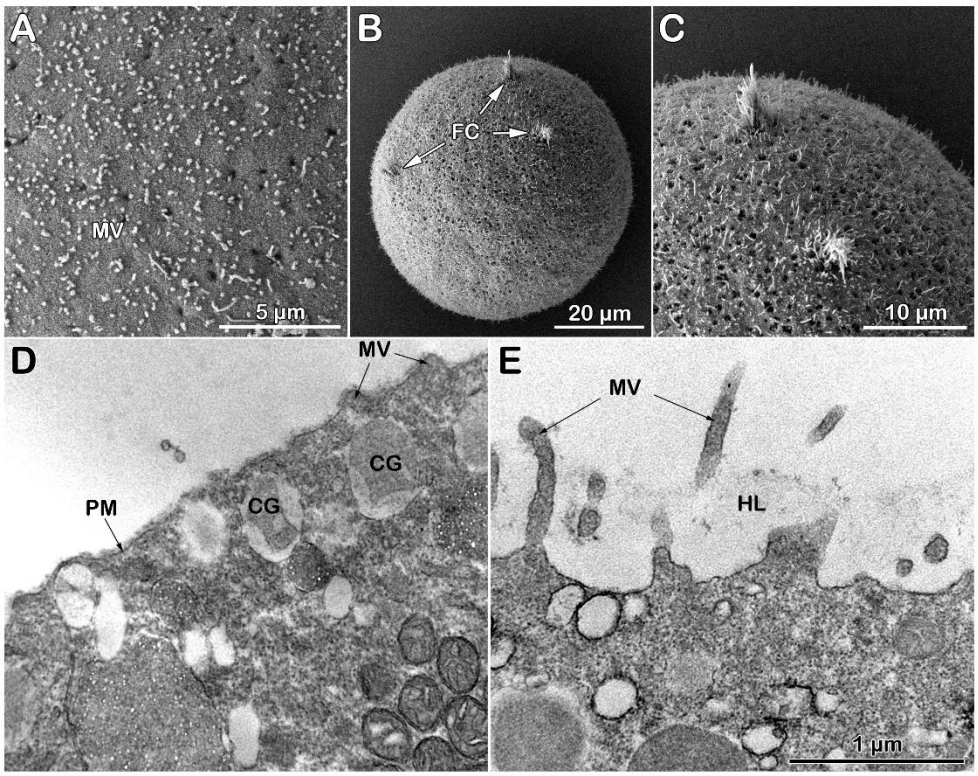

Figure 6. Scanning and transmission electron micrographs of the denuded *P. lividus* eggs at fertilization. (**A**) The surface of an egg after the removal of VL. This treatment decreases the number of microvilli (MV) and alters their morphology. (**B**) Inseminating denuded eggs leads to polyspermic fertilization, as evidenced by the formation of three fertilization cones (FC, arrows) that incorporate sperm. (C) Magnified image of the fertilization cones in panel B. Note the elongated MV in areas of the egg's surface where they were present before fertilization amid numerous interspersed holes. Note also that the FE elevation is absent because the VL had been removed before insemination. (**D**) The transmission electron micrograph shows the lack of the VL and the

 doi:10.20944/preprints202506.0164.v1

altered morphology of MV and cortical granules (CG). (**E**) Five minutes post-insemination, the micrograph shows the absence of the CG due to the exocytosis of their content and MV elongation on the surface. HL= Hyaline layer.

More dramatic effects of Con A on denuded eggs become particularly evident after fertilization. The SEM micrograph in Figure 7 A shows the surface of a denuded egg treated with Con A (200 µg/ml) for 5 minutes, which appears similar to that of untreated denuded eggs (see Figure 6 A for comparison). In contrast, the Con A-pretreted denuded eggs manifested changes in the fertilization cone (FC) structure after sperm penetration and nearly complete inhibition of MV elongation (Figure 7 B and C), indicating significant modifications of the structural plasticity of the MV on the egg surface caused by Con A pretreatment. Indeed, rather than elongating, as seen in untreated denuded eggs (see Figure 6 E), many MV collapsed, forming enlarged spherical tips. This striking change results from depolymerizing the actin filaments that shape MV [60].

The effects of Con A treatment on denuded eggs have been verified at an ultrastructural level, particularly in terms of the changes in MV and cytoplasmic morphology. The TEM micrograph shown in Figure 7 D illustrates the plasma membrane on the surface of a denuded egg that lacks the VL, with cortical granules (CG) located beneath the egg plasma membrane. After exposure to Con A, the denuded eggs exhibit more extraction and damage in their cytoplasm compared to the ultrastructure of the control (see Figure 6 D for comparison).

In denuded eggs fertilized after Con A pretreatment, alterations in the structural organization of the egg cortex were evident. Specifically, this treatment inhibited exocytosis of the CG, which remained beneath the egg plasma membrane even five minutes after insemination; the matrix of the CG was less electron-dense in TEM. The results of TEM further confirmed the finding with SEM regarding the changes in microvillar morphology induced by Con A. Instead of elongating on the surface of the activated egg, the microvilli of the unfertilized denuded eggs underwent significant flattening (see Figure 7 E).

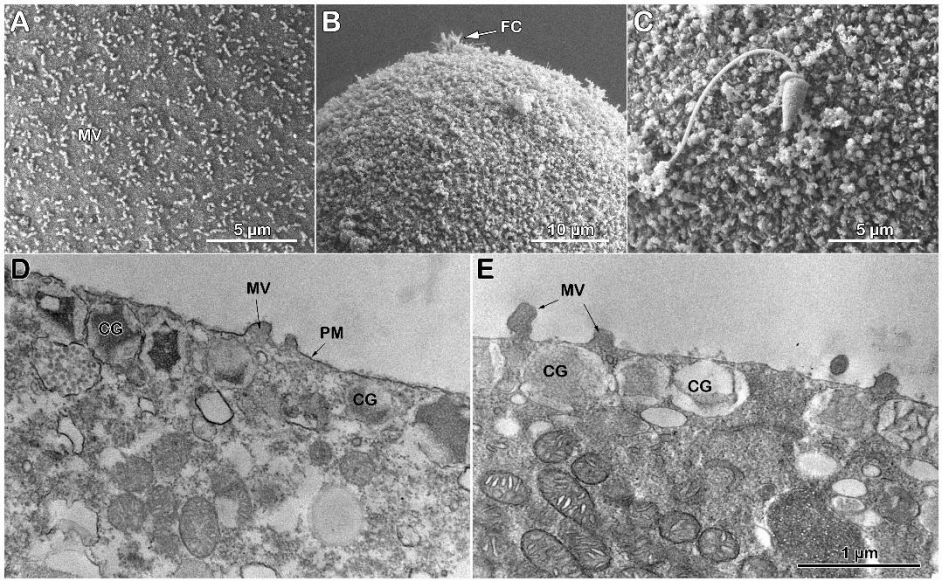

Figure 7. Effect of Con A on the fertilization of the denuded eggs of *P. lividus*. (**A**) The scanning electron micrograph of the denuded eggs exposed to Con A reveals the reduced number of microvilli (MV) and altered surface morphology. (**B**) Insemination of Con-A-treated denuded eggs results in modified fertilization cones (FC). (**C**) A higher magnification of the micrograph presented in B shows a significant lack of MV elongation and flattened microvilli (MV) on the egg surface. (**D**) A transmission electron micrograph of a denuded egg treated with Con A before insemination displays the altered morphology of microvilli (MV), cortical granules (CG), and cytoplasmic ultrastructure. (**E**) After insemination, the presence of CG beneath the plasma membrane was still evident on the surface of the activated egg five minutes after insemination. Additionally, MV are

 doi:10.20944/preprints202506.0164.v1

consistently flattening. Note the absence of FE elevation due to removing the vitelline layer from the unfertilized egg.

3.3. Alteration of the cortical F-actin in intact and denuded sea urchin eggs in response to Con A

The exposure of *P. lividus* eggs to Con A led to changes in the structural organization of the egg surface and cortex, as observed through electron microscopy. Furthermore, the finding that preincubation of the eggs to con A before insemination blocked sperm entry, which is often linked to F-actin, prompted an investigation into the effects of lectin treatment on the dynamics of the cortical actin cytoskeleton [26,29,34]. Preincubation of the intact eggs with Con A before fertilization had a visible impact on the structural changes of the eggs at the plasma membrane and the actin filaments (Figure 8). To visualize such changes, intact eggs were microinjected with bacterially expressed LifeAct-GFP and FM 1-43 membrane dye (Figure 8 A).

One minute after sperm was added, the FE elevated over the entire surface of the inseminated egg, resulting from the exocytosis of CG. The formation of F-actin spikes previously visualized with the LifeAct-GFP [30] in the perivitelline space (PS) beneath the FE was also observed with FM 1-43, the membrane dye (Figure 8 A). Five minutes post-insemination, a thicker layer of F-actin was uniformly distributed in the cortical region of the zygote, along with the development of a fertilization cone at the site of sperm entry, indicated by the arrow. When these eggs were preincubated with Con A for 5 min before insemination, the cortical reaction was subtly altered (Figure 8 B). The simultaneous visualization of the VL, stained red with Fluor Con A, alongside F-actin, marked in green with LifeAct-GFP (right panel), reveals a dimple on the zygote surface (Figure 8 B). This structure typically disappears in the control eggs at fertilization as the FE is elevated. However, in the eggs fertilized after the 5-minute preincubation with Con A, this dimple remained visible even five minutes after insemination, which is attributed to a significant delay in the contraction of eggs pretreated with the lectin. Furthermore, exposure of intact unfertilized eggs to lectin inhibits the separation and propagation of the VL, an effect also observable in light microscopy (Figure 1). Additionally, eggs treated with the fluorescent lectin before fertilization display abnormal F-actin polymerization, as detected by the LifeAct-GFP marker.

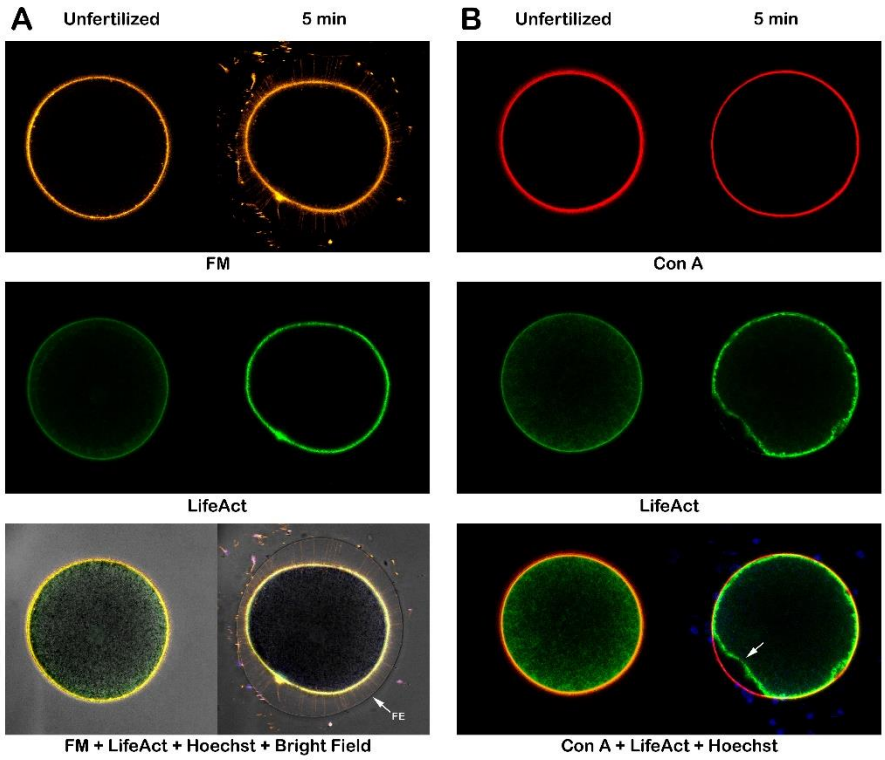

 doi:10.20944/preprints202506.0164.v1

Figure 8. Cortical reaction and F-actin changes in intact *P. lividus* eggs at fertilization. Intact eggs were incubated with or without Con A preincubation before insemination: (A) confocal microscopic images of the control eggs without Con A preincubation before and after insemination, (B) eggs with Con A preincubation (200 µg/ml, 5 min). To visualize the changes in the plasma membrane, F-actin, and the extracellular matrix, the same eggs were first microinjected or incubated with the corresponding fluorescent markers, as was described in the materials and Methods: FM 1-43 (orange color), LifeAct-GFP (green), and Alexa-Con A (red). Note that Con A preincubation inhibited the propagation and FE elevation. It is important to note that the reversible dimple formation (arrow) in control eggs is still visible on the surface of Con A-treated eggs 5 minutes after insemination. The fluorescent sperm were stained with the DNA dye Hoechst 33342.

Exposure of denuded eggs to Con A before insemination did not prevent multiple sperm from binding and fusing onto the egg membrane, as previously shown [26,30]. The confocal images (Figure 9) depicting the cortical response of denuded eggs before and after Con A treatment (200 µg/ml for 5 minutes) indicated that insemination does not cause these eggs to contract, which in intact eggs would typically lead to transitory formation of the dimple following sperm stimulation. Additionally, there is a noticeable absence of separation of the VL since it has already been stripped off from the eggs.

Moreover, the contents of cortical F-actin, which polymerizes by 5 min post-insemination, is slightly lower in denuded eggs when compared with the intact eggs (Figure 8). Regarding the binding of the lectin to the egg plasma membrane, the fluorescence visualization of Con A did not reveal significant alterations of the structural organization of the egg surface that was detected by electron microscopy observations (Figure 7). This discrepancy may be attributable to the lower resolution of the confocal microscope.

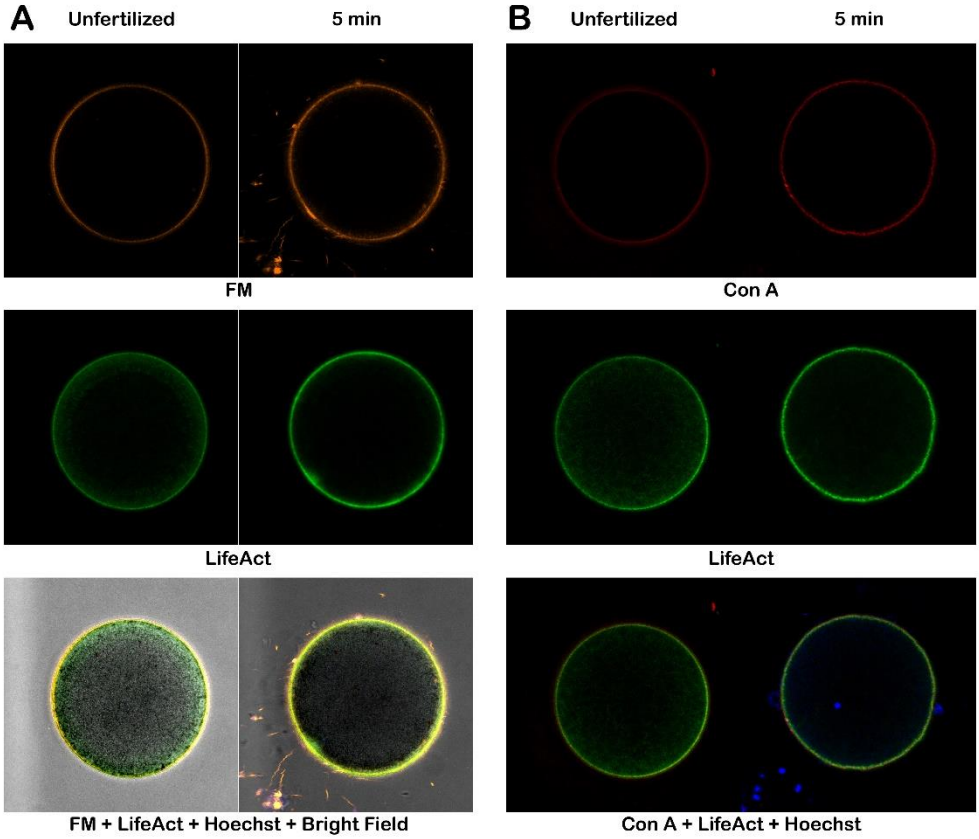

Figure 9. Con A pretreatment alters the cortical reaction of denuded *P. lividus* eggs at fertilization. Denuded eggs were incubated with or without Con A prior to insemination. To visualize the plasma membrane, F-actin, and the extracellular matrix, the same eggs were first microinjected or incubated with the corresponding fluorescent markers, as described in the Materials and Methods: FM 1-43 (orange), LifeAct-GFP (green), and Alexa-Con A

 doi:10.20944/preprints202506.0164.v1

(red). (**A**) Confocal microscopic images of the denuded eggs without Con A pretreatment. (**B**) Denuded eggs fertilized after 5 min incubation with 200 µg/ml. Blue signals represent sperm stained with Hoechst 33342.

While the elevation of the FE is a prominent late morphological event in a fertilized egg, the cortical actin filaments also undergo polymerization and seemingly centripetal translocation [61]; the latter cytoskeletal change starts approximately 10 minutes after insemination, which can be most easily visualized by injecting fluorescent phalloidin (Alexa Fluor 568 phalloidin) into the cytoplasm of unfertilized eggs at a final concentration of 10 µM (Figure 10 A). At this low concentration, the fluorescent phalloidin does not interfere with the physiological changes of the cortical F-actin, as was previously demonstrated [25,29,62]. When intact eggs were exposed to Con A before insemination, not only did the VL fail to separate from the egg surface, but the contractility of the egg cortex appeared to change. As a result, a modest dimple (Figure 10 B, arrow) remained on the surface of the egg for 20 minutes. Furthermore, Con A pretreatment altered the aforementioned centripetal mobilization of the F-actin (Figure 10 B). These findings suggest that the lectin binding on the egg extracellular matrix may have transmitted a certain signal to interfere with intracellular mechanisms by which actin filaments are reorganized in the fertilized eggs.

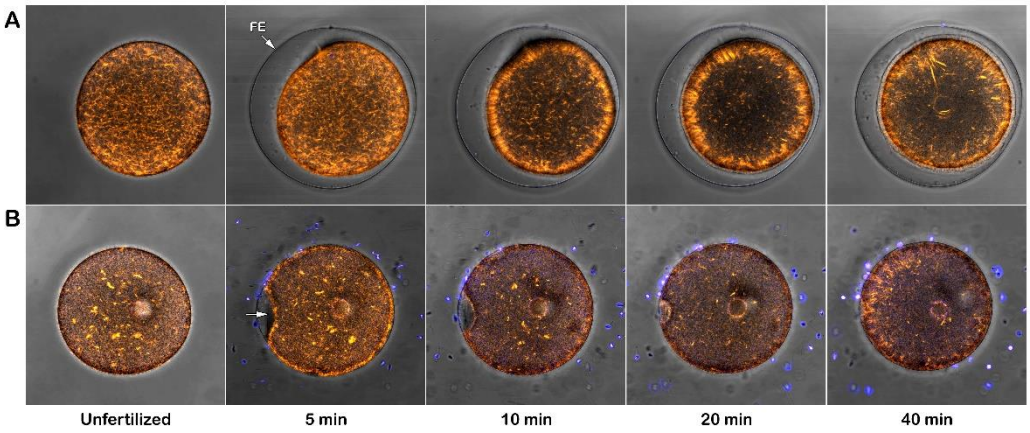

Figure 10. Effect of Concanavalin A (Con A) at a concentration on the fertilization reaction of intact *P. lividus* eggs microinjected with AlexaFluor 568–phalloidin. In the upper panel, a control egg's fertilization response shows the FE elevation following the exocytosis of cortical granules and a centripetal movement of actin filaments from the surface toward the center of the zygote. However, preincubation of the eggs with Con A (200 µg/ml, 5 min) inhibited the progressive reorganization of F-actin seen in the intact control eggs. Note the dimple (arrow) on these eggs that remained 5 to 20 min due to the decreased egg surface contractility caused by Con A.

3.4. Con A binding to the egg surface affects sperm-induced Ca^{2+} signals in intact and denuded eggs

The jelly coat (JC) and vitelline layer (VL) are stained with the Concanavalin A conjugated with Alexa Fluor 633 (Figs. 3 and Fit 11). It is widely accepted that the components of the extracellular structure surrounding the egg are critical in initiating the sperm acrosome reaction (AR), a species-specific sperm egg recognition and binding process prerequisite for fertilization. In other words, it is thought that JC and VL are required for sperm activation. However, our previous research on the sperm-induced Ca^{2+} response in *P. lividus* eggs has shown that sperm diluted in seawater can fertilize intact eggs, even when the structural integrity of the JC and VL is compromised or after their removal. Indeed, eggs deprived of JC and VL shown in Figure 11 C can still be fertilized by sperm solely diluted in seawater [26,29,30]. These results may be due to a small percentage (from 3 to 8%) of the ready-made sperm known to be present in the sperm population [63]. To test if some sea urchin sperm diluted with seawater already bear morphological differences, we stained fresh living sperm in seawater with the fluorescent polyamine BPA-C8-Cy3 [29]. Visualization of the fluorescent staining of sperm evidenced the presence of a structural protrusion (Figure 9 A, arrowheads) on the tip of

 doi:10.20944/preprints202506.0164.v1

many sperm heads, resembling a sort of acrosomal process. However, the length of such sperm protrusion is much shorter than that of the sperm AR induced in vitro by the JC or at high pH and visualized with light and electron microscopy [19,64–67] but more similar to that of the sperm observed by SEM on the surface of *P. lividus* eggs fertilized under physiological conditions [68].

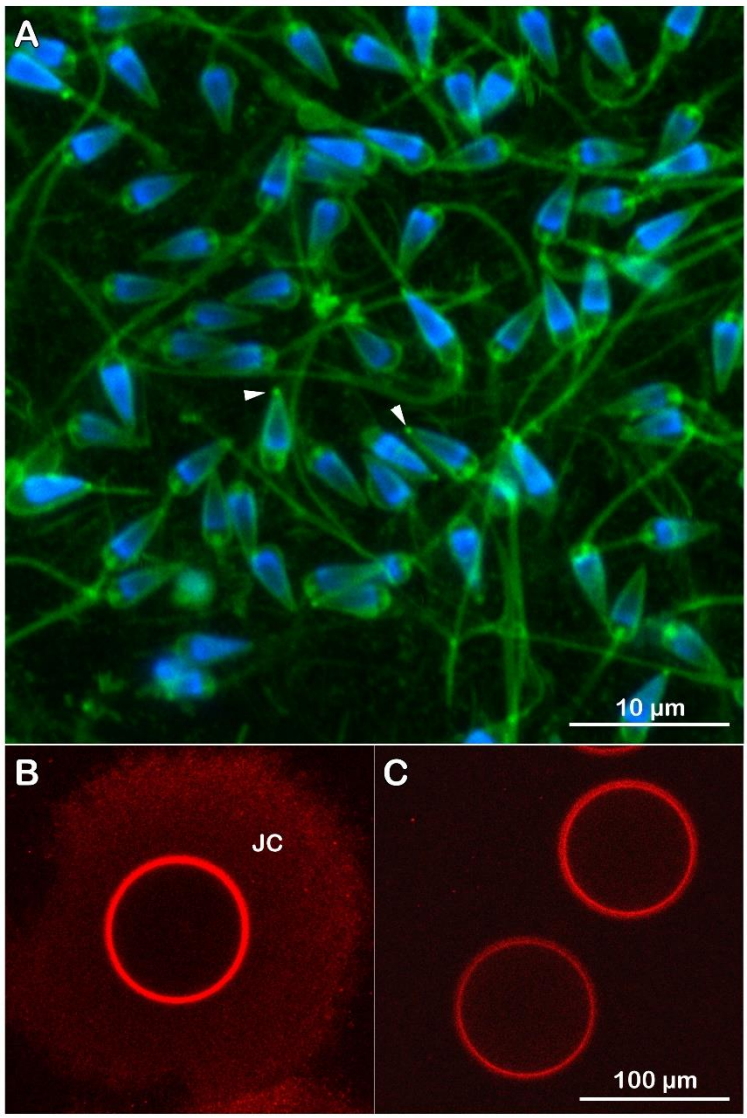

Figure 11. (**A**) The staining of living *P. lividus* sperm diluted with the fluorescent polyamine BPA-C8-Cy3 in natural seawater (NSW). Note the presence of membrane protrusions on the sperm head, which resemble an acrosomal process (indicated by arrowheads). (**B**) Intact eggs were stained with Alexa Fluor 633-Con A to visualize JC and the VL. (C) Denuded eggs stained with Con A. The sperm diluted in NSW are able to fertilize both intact and denuded eggs, raising the question about the indispensability of egg jelly-induced AR for fertilization.

The significant changes in the morphology of microvilli and cortical granules (CG) observed in *P. lividus* eggs exposed to Con A visualized with electron microscopy raised questions about how these effects of the lectin might interfere with sperm-induced Ca^{2+} signals, which are influenced by the alterations in the egg surface and cortex [26,31,38]. Therefore, we monitored the sperm-induced Ca^{2+} signals in intact and denuded unfertilized eggs exposed to non-fluorescent lectin before insemination.

The graphs in Figure 12 illustrate the Ca^{2+} signals produced in intact *P. lividus* eggs that were fertilized after preincubation with various doses of Con A. In intact eggs not treated with the lectin (green lines), a few seconds after the addition of sperm, a simultaneous release of Ca^{2+} (cortical flash,

 doi:10.20944/preprints202506.0164.v1

CF) occurs in the cortical region of the activated egg, which depends on the length and morphology of the microvilli, as previously shown by our results [26,31,38]. The CF, with an amplitude of 0.064 ± 0.007 RFU (n= 10 eggs), is followed by a Ca^{2+} wave (CW), which starts at the site on the egg surface where the sperm fuses with the egg's plasma membrane. The time interval between the two Ca^{2+} events, referred to as the 'latent period', is approximately 6.7 ± 0.6 seconds (n=10 eggs), measuring with the onsets of the CF and CW. The CW reaches an amplitude of 0.34 ± 0.02 RFU (n=10 eggs), and the Ca^{2+} signal propagates to the opposite pole (traverse time) of the egg in about 20 sec. The time-lapse movie in Supplementary Video 1, captured by simultaneous CCD camera recordings, also showcases the structural changes in the cortical region of intact eggs not exposed to Con A, along with the concomitant fluctuations of Ca^{2+} signals following fertilization. In this video, sperm binding upon its arrival site on the egg surface was set as t= 0. Two seconds later, a simultaneous increase in Ca^{2+} is observed in the cortex under the entire egg surface (CF). Approximately six seconds after sperm binds to the egg, a CW is initiated (see also Supplementary Figure 2 for the measurement parameters used to assess the sperm-induced Ca^{2+} response and the histograms shown in Figure 13). The release of intracellular Ca^{2+} triggers the contraction of the egg's surface, forming a dimple-like structure that facilitates the separation of the vitelline layer from the egg plasma membrane. This separation progresses across the entire surface of the egg over about one minute, triggering CG exocytosis and thereby forming a thick fertilization envelope.

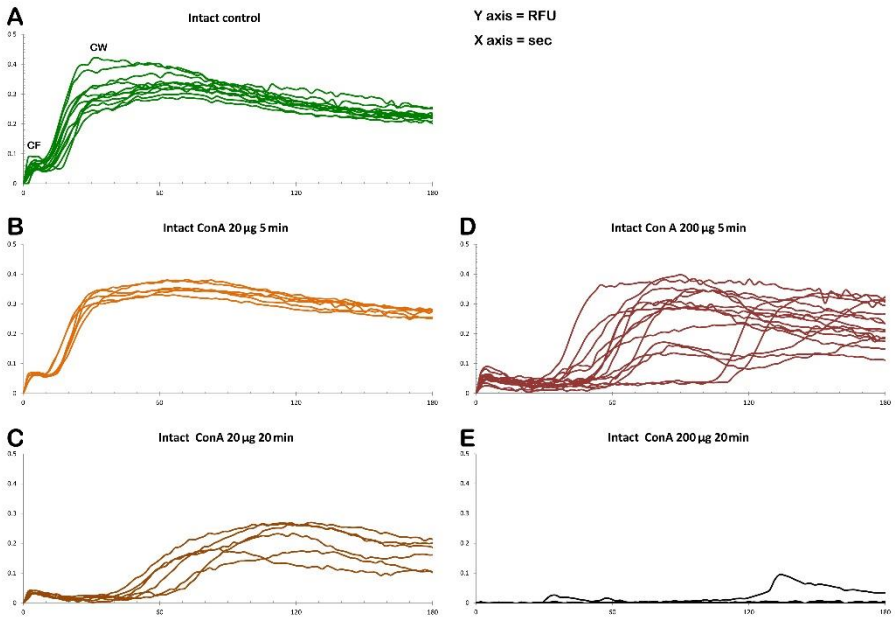

Figure 12. Effect of Con A on the fertilization Ca^{2+} response. Intact *P. lividus* eggs microinjected with calcium dyes were preincubated with various doses of Con A for 5 min before fertilization. The relative fluorescence (RFU) of the Ca^{2+} signal was obtained from a time-lapse recording after sperm addition. The moment of the first Ca^{2+} signal was set as t = 0. **A**) The intact (not treated, control) eggs fertilized in NSW at pH 8.1 exhibited two modes of Ca^{2+} responses: the cortical flash (CF) and the subsequent Ca^{2+} wave (CW). The time interval between the two events is referred to as the 'latent period.' (B-E) When intact eggs are exposed to various concentrations of Con A, there is a significant prolongation of the latent period and an alteration of the patterns of the sperm-induced Ca^{2+} response, as shown in the histograms in Figure 13.

 doi:10.20944/preprints202506.0164.v1

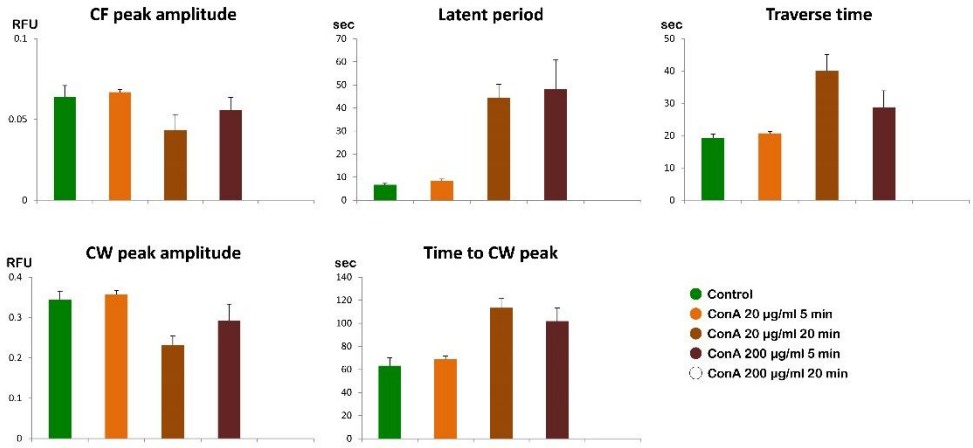

Figure 13. Histograms summarizing the Ca^{2+} response in intact (control) and treated *Paracentrotus lividus* eggs at fertilization. Before insemination, the eggs were incubated with various doses of Con A.

The examination of the intact eggs preincubated to Con A revealed that, regardless of the lectin concentration being used (1 µg to 1 mg/ml for 5 minutes), sperm physiology remained unaffected, as indicated by the unchanged time required by the fertilizing sperm to initiate the CF (data not shown). However, aside from this parameter, the graphs and histograms presented in Figure 12 and 13 showed significant differences in the patterns of Ca^{2+} signals displayed by the fertilized eggs inseminated after a 5 min preincubation with 200 µg/ml of Con A, regardless of whether or not Con A was removed from NSW before the insemination. The hallmark of the Ca^{2+} response in the intact eggs fertilized after Con A pretreatment was that there was a remarkably delayed initiation of the CW after the occurrence of the CF (Figure 12 and 13). Thus, the latent period in these eggs was significantly prolonged to 48.1 ± 12.6 sec (n = 15) compared with the control eggs not pretreated with Con A (6.7 ± 0.6 sec, n = 10, $p < 0.01$). The exposure of unfertilized intact eggs to this concentration of lectin before fertilization also influences the timing when the CW reached its peak intensity, which was measured at 101.9 ± 11.5 sec (n = 15), as opposed to 63.3 ± 6.7 sec (n = 10, $p < 0.01$). In the treated group, the amplitude of the CW was significantly lower, measuring 0.29 ± 0.04 RFU, compared to the control group (0.34 ± 0.02 RFU, n=10, $p < 0.05$). Additionally, the propagation of the CW from its initiation point (sperm egg fusion site) to the antipode of the Con A-pretreated eggs (i. e., traverse time) was significantly delayed (28.7 ± 5.1 sec, n=15, in comparison with the control eggs 19.3 ± 1.1 sec, n=10, $p < 0.05$). This is illustrated in the brown curves in Figure 12 and the histograms in Figure 13. Furthermore, overlay imaging of the egg morphology and Ca^{2+} signals in the Con A-pretreated eggs at fertilization highlights not only a significantly prolonged latent period before the onset of the CW but also the delayed separation of the VL. Moreover, the VL separation does not propagate across the entire surface (Supplementary Video 2).

The graphs and histograms presented in Figure 12 and 13 illustrate a time-dependent effect of lectin on the fertilization response of *P. lividus* eggs when exposed to a lower concentration of Con A (20 µg/ml). Specifically, a 5-min pretreatment did not significantly affect the sperm-induced Ca^{2+} signals compared to the fertilization Ca^{2+} response in the untreated eggs. In contrast, in the eggs pretreated with the same dose of Con A for 20 min, the fertilization Ca^{2+} response was significantly altered, as indicated by the graphs in Figure 12 (orange lines) and the histograms in Figure 13.

The graphs shown in Figure 14 (A and B) illustrate the Ca^{2+} signals in the intact and denuded eggs at fertilization. Although being deprived of VL and JC, denuded eggs washed several times in NSW at pH 8.1 were all able to be fertilized by sperm and produced apparently normal Ca^{2+} wave (Figure 14 B, blue lines) with a CF average amplitude noticeably reduced: 0.052 ± 0.003 RFU (n=13 eggs) as opposed to 0.064 ± 0.007 RFU for the intact eggs (n = 10 eggs, $p < 0.05$). On the other hand,

 doi:10.20944/preprints202506.0164.v1

other aspects of the Ca2+ responses in denuded eggs were virtually the same as those of the intact eggs: i) the average latent period for the denuded eggs was 5.7 ± 0.7 sec (n= 13), while that of the intact eggs was 6.7 ± 0.6 seconds), ii) average amplitude of the denuded eggs (0.33 ± 0.01 RFU, n = 13) was practically the same as that of the intact eggs (0.34 ± 0.02 RFU, n=10), iii) the traverse of the denuded eggs (19.3 ± 1.1 sec, n = 10) was again not significantly different from that of the intact eggs (20.3 ± 1.5 sec, n = 13).

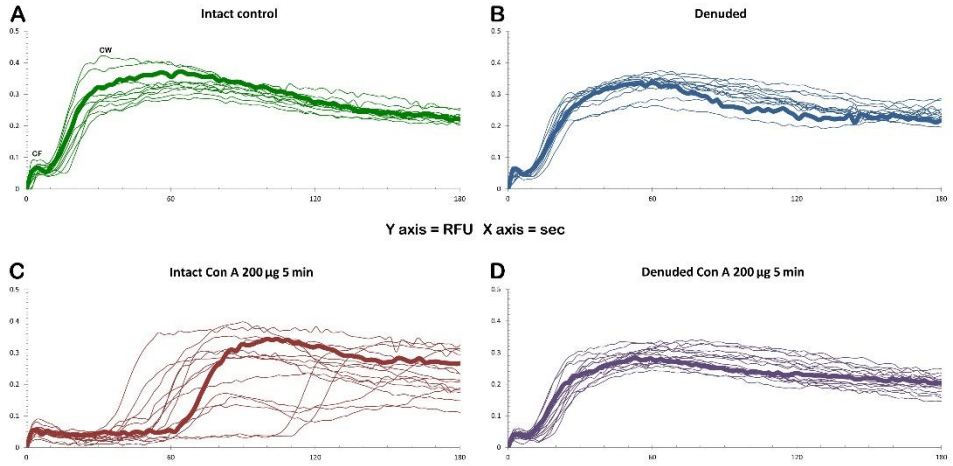

Figure 14. Effect of Con A on the fertilization Ca^{2+} response in intact and denuded *P. lividus* eggs. **A)** The graphs show the relative fluorescence (RFU, green curves) recorded in the intact (untreated) and denuded (blue lines, **B**) eggs in natural seawater (NSW) without Con A preincubation. The moment of the first detectable Ca^{2+} response (CF) was set as t=0. (**C**) Intact eggs preincubated with 200 µg/ml for 5 min before insemination (purple curves). (**D**) Denuded eggs were inseminated after 5 min preincubation with 200 µg/ml (violet curves). Note that the Con A pretreatment significantly prolongs the latent period in the intact eggs at fertilization but not in the denuded eggs. The bolded curves represent the graphs of the Ca^{2+} responses of the eggs shown in the Supplementary Videos.

Monitoring the morphological changes at fertilization, subtle differences were observed between denuded and intact eggs (Supplementary Video 3). According to the bright field images, activation of the denuded eggs by sperm did not trigger the formation of the dimple-like structure at the site of sperm fusion after the propagation of the CW. By contrast, the intact eggs at fertilization exhibited the characteristic dimple-like structure after the CW swept away from the sperm fusion site (see Supplementary Video 1). The time-lapse video 3 also revealed the lack of separation of the VL from the egg surface because it had been removed before insemination. A comparison of the parameters characterizing the pattern of the sperm-induced Ca^{2+} signals between denuded eggs fertilized after the pretreatment with Con A at a concentration of 200 ug/ml and 5 minutes (Figure 14, purple curves) showed that the amplitudes of both CF and CW were significantly reduced as a result of the Con A pretreatment. Whereas CF without Con A reached 0.052 ± 0.003 RFU, n =13), the Con A pretreatment lowered the CF amplitude to 0.044 ± 0.005 RFU (n = 16, $P < 0.01$). Likewise, the amplitude of the CW was reduced from 0.33 ± 0.01 RFU (without Con A, n = 13) to 0.27 ± 0.03 RFU (n = 16 eggs, $p < 0.01$) as a result of Con A pretreatment before insemination (see also the Supplementary Video 4).

4. Discussion

Fertilization of sea urchin eggs has been extensively studied across numerous species for over a century, resulting in a vast body of literature. Key findings indicate that fertilization is regulated by three significant interactions between the sperm and the egg. First, when the sperm contacts the outer jelly coat (JC) of the egg, the sperm acrosome reaction (AR) is triggered. This reaction is essential for forming the F-actin-linked acrosomal process (AP) extending from the head of the sperm, which

 doi:10.20944/preprints202506.0164.v1

exposes the adhesive protein bindin. Second, the adhesive protein bindin on the AP attaches explicitly to the glycoprotein of the vitelline layer (VL) that tightly covers the microvilli (MV) of the egg membrane. Finally, the fusion of the sperm with the egg membrane transduces the fertilization response, which is regulated by electrical changes of the egg membrane and Ca^{2+} signals concomitant with the exocytosis of the cortical granules (CG). The contents of the CG released between the VL and egg plasma membrane separate them by expanding the perivitelline space. The VL develops into the thick FE, which hardens by crosslinking [56,69,70]. It has been shown that upon insemination of sea urchin eggs, both the JC and VL play vital roles in sperm and egg activation. Furthermore, it has been postulated that the early changes of the egg membrane potential (depolarization) at the moment of the gamete fusion serve as an electrically mediated fast mechanism to block the attachment of multiple sperm, thereby preventing polyspermy at fertilization [71].

Our recent findings, however, have challenged the prevailing view on how sperm fertilizes sea urchin eggs by demonstrating the following key points. First, sperm can activate *P. lividus* eggs without undergoing the JC-induced AR. Second, species-specific recognition between gametes may occur at the level of the egg plasma membrane rather than at the VL. These results are evident because denuded eggs, which lack both the VL and JC, undergo polyspermic fertilization through the binding and fusion of multiple sperm [26,30 and Figure 6]. Finally, the fast block to polyspermy may be mediated structurally rather than electrically. This structural response involves adequately organizing F-actin-linked structures on the surface of unfertilized eggs, playing a crucial role in ensuring that only one sperm successfully activates the egg [25,42,72].

In addition to being the location of the sperm receptor's extracellular domain, which recognizes the bindin exposed on the AP of the sperm, the VL supposedly plays a crucial role in preventing the binding of multiple sperm through a slow mechanical block to polyspermy. At fertilization, during the release of CG content in the perivitelline space, a protease modifies the structure of the VL, causing the bound sperm to detach. The subsequent complete swelling of the VL over the entire zygote surface, leading to the formation of the FE, mechanically prevents any further interactions with additional sperm [15,16,73,74].

Contrary to the prevailing view, this study confirms our earlier findings that the VL of unfertilized eggs may hide regions on the egg plasma membrane where multiple sperm could attach, provided that the structural integrity of the VL is compromised [29,31]. Our findings regarding the significance of the morpho-functionality of the surface of unfertilized eggs, derived from their optimal physiological conditions, align with earlier observations from sea urchin fertilization studies [75]. These studies claimed that sea urchin eggs "…….*if in best conditions are never polyspermic …… Normally monospermic eggs can be rendered polyspermic by experimental treatment…..*" [76], which was corroborated in later studies [29,34,39]. A recent proposal suggests that the intact structure of the VL in unfertilized eggs is crucial for the fertilization process. This glycoprotein structure surrounding microvilli facilitates the fusion of only the fertilizing sperm with the egg membrane at a specific site not masked by the VL [26].

In addition to using lectins as markers for the surface architecture of normal and malignant cells in culture, Con A has been shown to specifically bind to the carbohydrate residues of the glycocalyx and cell membranes. Research has demonstrated that Con A inhibits various modification events at the surface of fertilized sea urchin eggs, including forming the fertilization envelope when eggs are inseminated after exposure to the lectin. This inhibition has been interpreted as a blockage of fertilization and subsequent cleavage [14,53,54,57].

In this study, we examined the effects of Con A on the fertilization of *P. lividus* eggs, aiming to resolve conflicting data in the literature regarding the role of glycoprotein components of the VL in the context of sperm egg recognition and binding. Using fluorescent Con A, our study also explored lectin binding to identify the glycoconjugates on the surface of intact and denuded eggs from which the VL had been stripped off. The results have confirmed Con A binding sites on the VL of intact eggs and, for the first time, on the JC surrounding them. In intact eggs, although the binding of Con A to the VL inhibits its separation across the entire surface of the egg, the sperm still triggered the

 doi:10.20944/preprints202506.0164.v1

fertilization Ca^{2+} signal transduction. This finding contrasts with previous studies reporting that Con A treatment of unfertilized (intact) eggs inhibits the elevation of the FE and, consequently, fertilization. In this study, we analyzed the extent of inhibition by measuring early fertilization events, including the pattern of sperm-induced Ca^{2+} signals upon fusion between the two gametes and the number of sperm incorporated into the egg. The results indicate that, despite changes in the morphology of the egg surface and cortical region, a modified fertilization response can still be triggered in the eggs that were inseminated after Con A preincubation. This study demonstrates that Con A binding to the extracellular matrix leads to altered cortical responses of the egg at fertilization, manifesting as significantly impaired sperm-induced Ca^{2+} signals and sperm incorporation. Alteration of the extracellular matrix by Con A binding affects the structure and dynamics of the F-actin comprising the egg's surface and cortical region, as judged by TEM and confocal microscopy utilizing LifeAct-GFP.

Exposure to Con A causes morphological changes in the VL and the F-actin-containing MV in intact eggs, to which the VL tightly adheres. These structural changes, which prevent the separation of the VL from the egg plasma membrane, are evident in the retention of cast remnants from the tips of the MVs that are still observed five minutes after insemination, as shown in the electron microscopy images (Figure 5 and Supplementary Video 2). The Con A treatment affecting proper detachment of the VL from the egg membrane in response to sperm stimulation may be related to the extended latent period experienced by eggs exposed to the lectin before insemination (see the graphs in Figure 12 and Supplementary Figure 2 for the measurement parameters of the Ca^{2+} signals at fertilization).

In line with the crucial role of the VL detachment from the egg membrane in regulating the initiation of the CW, we found that Con A pretreatment prolongs the latent period of the Ca^{2+} response in the intact eggs but not in the denuded eggs (Figure 14). Interestingly, a delayed CW onset after the CF is consistently observed in *P. lividus* eggs inseminated after incubation with actin drugs such as cytochalasin B and latrunculin A [34]. These findings are consistent with electrophysiological measurements reported in previous studies. Specifically, during fertilization in the eggs of the sea urchin species used in our experiments, two electrical events occur across the egg plasma membrane in response to the interaction with the fertilizing sperm. The first event is a step-like depolarization a few seconds after insemination, followed by a fertilization potential (FP) with a latent period between these two electrical changes of approximately 11 seconds [32,33]. Hence, at fertilization, the actin cytoskeletal changes at the sea urchin egg surface underlie the alteration of the Ca^{2+} response (prolonged latent period) in these eggs, and the Ca^{2+} response is precisely mirrored by the electrophysiological one [34,37,77]. While it has been postulated that the Ca^{2+} influx during the latent period is crucial for the initiation of the CW [78], it has been suggested that the polymerization status of the F-actin bundles within the MV of the egg is an essential determinant of Ca^{2+} influx [79] with Ca^{2+} channels being located in the MV. Disruption of the actin filaments with actin drugs also leads to the 'spontaneous' generation of Ca^{2+} influx and waves in starfish eggs [60]. Furthermore, the Con A pretreatment also modified the structure of the CG and how they are associated with the egg membrane (Figure 5). Because CG are connected to the PM via subplasmalemmal actin filaments and their disassembly contributes to shaping the Ca^{2+} wave patterns [36,38], the earlier observation that both the actin cytoskeleton at the egg surface and the CG influence the pattern of Ca^{2+} signaling in fertilized eggs suggest that the ultrastructural changed in the subplasmalemmal region introduced by Con A may play a crucial role in altering the fertilization Ca^{2+} events in these eggs [34,38].

Furthermore, the results of this study support our previous findings that the sperm of *P. lividus* can fertilize eggs without undergoing acrosome reaction (AR) by the JC, and that the sperm can achieve its goal of fertilizing denuded egg lacking the VL where the sperm receptor should be located [26,29,30 and Figure 6]. Additionally, the data of fluorescent Con A binding (Figure 3 and Figure 11) demonstrate that the egg membrane contains lower-affinity sites for the lectin when the JC and VL have been removed before insemination, similar to the earlier observations in other sea urchin species [54]. However, in contrast to the published data, our results show that the fluorescence from the lectin

 doi:10.20944/preprints202506.0164.v1

bound to the membrane of denuded eggs after insemination does not reveal an increase in the number of binding sites following the exocytosis of CG, indicating that new membranes are not inserted into the egg membrane after CG exocytosis as previously suggested [54]. Indeed, under our experimental conditions, we found that treating denuded eggs with Con A flattens the MV on the egg surface and impairs the process of CG exocytosis (Figure 7). Interestingly, in addition to reducing the number of sperm entry entries, denuded eggs exposed to Con A experienced a statistically significant lower CF and CW amplitude as a result of the CG exocytosis impairment, reinforcing the critical function of the microvillar and CG morphology in transducing the fertilization Ca^{2+} response in these sea urchin eggs. It follows that although several signaling pathways have been proposed to explain the complex systems of intracellular Ca^{2+} mobilization activated during the fertilization of sea urchin eggs [80–87], further studies are needed to uncover the molecular events involved in sperm-induced Ca^{2+} signaling.

Our results indicate that fertilization can still occur when sperm interacts with denuded eggs that have undergone significant changes in their MV morphology. These changes include a reduction in both the number and length of the MV (see Figure 4 and Figure 6 for a comparison with the control), which is attributed to the stripping of the vitelline layer (VL) [26,30]. It would be beneficial to understand whether, even under these conditions, the fertilizing sperm primarily fuses with the egg membrane at the tip of the microvilli, as suggested by previous ultrastructural analyses [19,72], or if this interaction occurs at other regions of the egg membrane [30]. Finally, our results support the notion that lectins inhibit cell migration by regulating F-actin content and distribution [88]. Understanding the molecular mechanisms that connect signaling molecules to the regulation of the actin cytoskeleton could provide a new perspective on the potential of Con A as a cancer cell killer [89].

Supplementary Materials: The following supporting information can be downloaded at the website of this paper posted on Preprints.org, Figure S1: Binding of Concanavalin A conjugated with Alexa Fluor 633 to the jelly coat and vitelline layer to intact *P. lividus* eggs pre-injected with the Ca^{2+} dye using a CCD camera. (**A**) Intact eggs. (**B**) Eggs from which the jelly coat (JC) and vitelline layer (arrow) had been removed. Note the absence of the JC and a lower signal of the egg surface due to the binding of the lectin to the egg plasma membrane. Figure S2: Parameters of the Ca^{2+} response in fertilized eggs of *P. lividus*: (**A**) The relative increase in fluorescence intensity compared to time 0. (**B**) The relative increase in fluorescence intensity compared to the preceding time point. Video S1: A time-lapse overlay showing the fertilization response of an intact egg of *P. lividus*, illustrating the simultaneous cortical reaction and Ca^{2+} signals. Two seconds after the fertilizing sperm fuses with the egg membrane, a cortical Ca^{2+} release, known as a cortical flash, occurs at the periphery of the activated egg. Six seconds later (i.e., "latent period"), a Ca^{2+} wave begins at the site of sperm-egg fusion and propagates to the opposite pole of the zygote within approximately 20 seconds. The propagation of this Ca^{2+} wave triggers contractions in the egg, resulting in a dimple at the site where the wave originates. This contraction separates the vitelline layer from the egg membrane, and the separation spreads across the entire surface of the zygote. Ultimately, this process leads to the full elevation of the fertilization envelope due to the exocytosis of cortical granules. Additionally, refer to the corresponding relative fluorescence graph in Figure 14 (bold green line) and the histograms in Figure 13, which analyze the parameters of the Ca^{2+} response pattern. Video S2 features a time-lapse overlay of the fertilization response of an intact *P. lividus* egg inseminated after Con A (200 µg/ml, 5 min) treatment, showcasing the cortical reaction and Ca^{2+} signals. The exposure of unfertilized, intact eggs to the lectin significantly compromises the fertilization response without completely blocking it. Unlike the non-treated eggs, eggs pretreated with Con A display a consistent delay of about one minute in initiating the Ca^{2+} wave following the onset of the cortical flash. This time lag markedly prolongs the latent period. Additionally, there is a noticeable delay in dimple formation due to the changes in the egg's contractility, which prevents the elevation of the fertilization envelope across the entire surface of the zygote. For further details, refer to the corresponding relative fluorescence graph in Figure 14 (the brown bold curve) and the histograms in Figure 13, which illustrate the alterations in the parameters of the Ca^{2+} response pattern. Video S3: A time-lapse overlay acquisition of the fertilization response of a denuded *P. lividus* egg to visualize the cortical reaction and Ca^{2+} signals. The binding

 doi:10.20944/preprints202506.0164.v1

of the fertilizing sperm to a denuded egg triggers a cortical flash two seconds later, leading to the initiation of a Ca^{2+} wave at the sperm-egg fusion site with a latent period of about six seconds, which is not significantly different from that observed in intact eggs. However, the spread of the Ca^{2+} wave does not induce zygote contraction, dimple formation, or the separation of the vitelline layer from the egg membrane due to its removal before insemination. For the correspondent relative fluorescence graph, refer to the blue bold line in Figure 14 and the analysis of other parameters related to the pattern of the Ca^{2+} fertilization response in the Results Section. Video S4: A time-lapse overlay acquisition of the fertilization response of a denuded *P. lividus* egg inseminated after Concanavalin A (200 μg/ml, 5 min) treatment. When exposed to the lectin, the fertilization response of a denuded egg shows no significant differences in the initiation of the Ca^{2+} wave (latent period) following the onset of the cortical flash. As for the untreated denuded eggs, the removal of the vitelline layer before insemination affects egg contraction, dimple formation, and the elevation of the fertilization envelope from the zygote surface. For further details, refer to the corresponding relative fluorescence graph in Figure 14 (purple bold line) and the analysis of other parameters related to the pattern of the fertilization Ca^{2+} response in the Results Section.

Author Contributions: Conceptualization, L.S., N.L. and J.T.C; and methodology, N.L., L.S. and M.P.; resources, L.S. and J.T.C.; formal analysis, N.L., L.S. and J.T.C.; data curation, N.L., L.S. and J.T.C.; visualization L.S., N.L. and J.T.C.; writing—original draft preparation, L.S.; writing—review and editing, L.S., J.T.C. and N.L.; supervision, L.S.; project administration, L.S. and J.T.C.; funding acquisition, L.S. and J.T.C. All authors have read and agreed to the published version of the manuscript.

Funding: This research received no external funding. This work was financially supported by the research fellowship to N.L. granted by the Stazione Zoologica Anton Dohrn for collaboration with L.S.

Institutional Review Board Statement: Sea urchins *P. lividus* used for the present study were collected according to the Italian legislation (DPR 1639/68, 19 September 1980 and confirmed on 1 October 2000). All the experimental procedures were carried out in accordance with the guidelines of the European Union (Directive 609/86).

Informed Consent Statement: Not applicable.

Data Availability Statement: Not applicable.

Acknowledgments: N.L. was supported by the research fellowship supported by the SZN institutional fund. The authors express their gratitude to the technicians at the Advanced Microscopy Center at SZN for fixing the samples for electron microscopy and assisting with the scanning electron microscope observations. Special thanks also go to Giovanni Gragnaniello for his help in preparing the Supplementary Videos and figures. Additionally, the authors would like to thank the Euro-BioImaging facility at the IEOMI (CNR) in Naples for assisting with cutting and staining ultrathin sections and facilitating observations with the transmission electron microscope. They are also grateful to Jean-Marie Lehn for providing the fluorescent polyamine BPA-C8-Cy3.

Conflicts of Interest: The authors declare no conflicts of interest.

References

1. Hirohashi, N.; Kamei, N.; Kubo, H.; Sawada, H.; Matsumoto, M.; Hoshi, M. Egg and sperm recognition systems during fertilization. *Dev. Growth Differ*. **2008**, 50, S221-S238. doi.org/10.1111/j.1440-169X.2008.01017.x
2. Dan, J.C. Studies on the Acrosome. I. Reaction to Egg-Water and Other Stimuli. *Biol. Bull.* **1952,** 103, 54-66. doi: 0.2307/1538405.
3. SeGall, G.; Lennarz, W.J. Chemical characterization of the components of the jelly coat from sea urchin eggs responsible for induction of the acrosome reaction. *Dev Biol.* **1979**, 71,33-48. doi: 10.1016/0012-1606(79)90080-0.
4. Alves, A.P.; Mulloy, B.; Diniz, J.A.; Mourão, P.A. Sulfated polysaccharides from the egg jelly layer are species-specific inducers of acrosomal reaction in sperms of sea urchins. *J Biol Chem* . **1997**, 272, 6965-71. doi: 10.1074/jbc.272.11.6965.

 doi:10.20944/preprints202506.0164.v1

5. Vacquier, V.D.; Moy, G.W. Isolation of bindin: The protein responsible for adhesion of sperm to sea urchin eggs. *Proc. Natl. Acad. Sci. USA* **1977**, 74, 2456–2460. doi: 10.1006/dbio.1997.8729.
6. Hirohashi, N.; Vacquier, V.D. High molecular mass egg fucose sulfate polymer is required for opening both Ca^{2+} channels involved in triggering the sea urchin sperm acrosome reaction. *J. Biol. Chem.* **2002**, 277, 1182-1189. doi: 10.1074/jbc.M108046200.
7. Neill, A.T.; Vacquier, V.D. Ligands and receptors mediating signal transduction in sea urchin spermatozoa. *Reproduction* **2004**, 127,141-149. doi: 10.1530/rep.1.00085.
8. Darszon, A.; Nishigaki, T.; Wood, C.; Treviño, C.L.; Felix, R.; Beltran, C. Calcium channels and Ca^{2+} fluctuations in sperm physiology. *Int. Rev. Cytol.* **2005,** 243,79-172. doi: 10.1016/S0074-7696(05)43002-8.
9. SeGall, G.K; Lennarz, W.J. Jelly coat and induction of the acrosome reaction in echinoid sperm. *Dev. Biol.* **1981**, 86, 87-93. doi.org/10.1016/0012-1606(81)90318-3.
10. Glabe, C.G.; Vacquier, V.D. Egg surface glycoprotein receptor for sea urchin sperm bindin. *Proc. Natl. Acad. Sci. USA* **1978**, 75, 881-885. doi.org/10.1073/pnas.75.2.881.
11. Kidd, P. The jelly and vitelline coats of the sea urchin egg: New ultrastructure features. *J. Ultrastr Res.* **1978**, 64, 204-215. doi.org/10.1016/S0022-5320(78)80038-0.
12. Chandler, D.E.; Heuser, J. The vitelline layer of the sea urchin egg and its modification during fertilization. A freeze-fracture study using quick-freezing and deep-etching. *J. Cell Biol.* **1980,** 84, 618–632. doi: 10.1083/jcb.84.3.618.
13. Glabe, C.G.; Grabel, L.B.; Vacquier, V.D.; Rosen, S.D. Carbohydrate specificity of sea urchin sperm bindin: a cell surface lectin mediating sperm-egg adhesion. *J. Cell Biol.* **1982**, 94, 123-8. doi: 10.1083/jcb.94.1.123.
14. Aketa, K.; Onitake, K.; Tsuzuki, H. Tryptic disruption of sperm-binding site of sea urchin egg surface. *Exp. Cell Res.* **1972**, 71, 27-32. doi.org/10.1016/0014-4827(72)90258-3.
15. Vacquier, V.D.; Epel, D.; Douglas, L.A. Sea urchin eggs release protease activity at fertilization. *Nature* **1972**, 237, 34-6. doi: 10.1038/237034a0.
16. Vacquier, V.D.; Tegner, M.J.; Epel, E. Protease activity establishes the block against polyspermy in sea urchin eggs. *Nature* **1972**, 240, 352-3. doi: 10.1038/240352a0.
17. Vacquier, V.D.; Payne, J.E. Methods for quantitating sea urchin sperm-egg binding. *Exp. Cell Res.* **1973**, 82, 227-35. doi: 10.1016/0014-4827(73)90265-6.
18. Carroll, E.J. Jr.; Epel, D. Isolation and biological activity of the proteases released by sea urchin eggs following fertilization. *Dev Biol*. **1975**, 44, 22-32. doi: 10.1016/0012-1606(75)90373-5.
19. Epel, D. The Program of Fertilization. *Sci. Am.* **1975**, 237, 128–138. doi:10.1038/scientificamerican1177-128.
20. Bryan, J. The isolation of a major structural element of the sea urchin fertilization membrane. *J. Cell Biol.* **1970,** 44, 635-644. doi.org/10.1083/jcb.44.3.635.
21. Kay, E.S.; Shapiro, B.M. Ovoperoxidase assembly into the sea urchin fertilization envelope and dityrosine crosslinking. *Dev. Biol.* **1987**, 121, 325-33. doi.org/10.1016/0012-1606(87)90168-0.
22. Larabell, C.; Chandler, D.E. Fertilization-Induced changes in the vitelline envelope of echinoderm and amphibian eggs: Self-assembly of an extracellular matrix. *J. Electron Microsc. Tech*. **1981**, 17, 294–318. doi:10.1002/jemt.1060170305.
23. Epel, D.; Weaver, A.M.; Mazia, D. Methods for removal of the vitelline membrane of sea urchin eggs: I. Use of dithiothreitol (Cleland Reagent). *Exp. Cell Res.* **1970**, 61, 64-68. doi.org/10.1016/0014-4827(70)90257-0.
24. Glabe, C.; Buchalter, M.; Lennarz, W.J. Studies on the interactions of sperm with the surface of the sea urchin eggs. *Dev. Biol.* **1981**, 84, 397-406. doi.org/10.1016/0012-1606(81)90408-5.
25. Limatola, N.; Vasilev, F.; Chun, J.T.; Santella, L. Sodium-mediated fast electrical depolarization does not prevent polyspermic fertilization in *Paracentrotus lividus* eggs. *Zygote* **2019**, 27, 1-9. doi.org/10.1017/S0967199419000364.
26. Limatola, N.; Chun, J.T.; Schmitt, J.-L.; Lehn, J.-M.; Santella, L. The Effect of Synthetic Polyamine BPA-C8 on the Fertilization Process of Intact and Denuded Sea Urchin Eggs. *Cells* **2024**, 13, 1477. doi.org/10.3390/cells13171477.
27. Wessel GM, Wada Y, Yajima M, Kiyomoto, M. Bindin is essential for fertilization in the sea urchin. *Proc. Natl. Acad. Sci. U.S.A.* **2021**, 118, e2109636118. doi.org/10.1073/pnas.2109636118.

 doi:10.20944/preprints202506.0164.v1

28. Hagström, B.E. Studies on the fertilization of jelly-free sea urchin eggs. *Exp. Cell Res*. **1956**, 10, 24-28. doi.org/10.1016/0014-4827(56)90066-0.
29. Limatola, N.; Chun, J.T.; Cherraben, S.; Schmitt, J.L.; Lehn, J.M.; Santella, L. Effects of Dithiothreitol on Fertilization and Early Development in Sea Urchin. *Cells* **2021**, 10, 3573. doi.org/10.3390/cells10123573.
30. Limatola, N.; Chun, J.T.; Santella, L. Species-Specific Gamete Interaction during Sea Urchin Fertilization: Roles of the Egg Jelly and Vitelline Layer. *Cells* **2022**, 11, 2984. doi.org/10.3390/cells11192984.
31. Limatola, N.; Chun, J.T.; Santella, L. Regulation of the Actin Cytoskeleton-Linked Ca^{2+} Signaling by Intracellular pH in Fertilized Eggs of Sea Urchin. *Cells* **2022**, 11, 1496. doi.org/10.3390/cells11091496.
32. Dale, B.; De Felice, L. J.; Taglietti, V. Membrane noise and conductance increase during single spermatozoon-egg interaction. *Nature* **1978**, 275,217-219. doi.org/10.1038/275217a0.
33. Dale, B.; Dan-Sohkawa, M.; De Santis, A.; Hoshi, M. Fertilization of the starfish *Astropecten aurantiacus*. *Exp. Cell Res*. **1981,** 132, 505–510. doi:10.1016/0014-4827(81)90132-4.
34. Chun, J.T.; Limatola, N.; Vasilev, F.; Santella, L. Early events of fertilization in sea urchin eggs are sensitive to actin-binding organic molecules. *Biochem. Biophys. Res. Commun.* **2014**, 450:1166-74. doi: 10.1016/j.bbrc.2014.06.057.
35. Spudich, A. Wrenn, J.T.; Wessells, N.K. Unfertilized sea urchin eggs contain a discrete cortical shell of actin that is subdivided into two organizational states. *Cell Motil. Cytoskel*. **1988**, 9, 85–96. doi:10.1002/cm.970090109.
36. Gillot, I.; Ciapa, B.; Payan, P.; Sardet, C. The calcium content of cortical granules and the loss of calcium from sea urchin eggs at fertilization. *Dev. Biol.* **1991**, 146, 396–405. doi:10.1016/0012-1606(91)90241-t.
37. Santella, L.; Limatola, N.; Chun, J.T. Calcium and actin in the saga of awakening oocytes. *Biochem. Biophys. Res. Commun*. **2015**, 460, 104–113. doi.org/10.1016/j.bbrc.2015.03.028.
38. Vasilev, F.; Limatola, N.; Chun, J.T.; Santella, L. Contributions of suboolemmal acidic vesicles and microvilli to the intracellular Ca^{2+} increase in the sea urchin eggs at fertilization. *Int. J. Biol. Sci.* **2019**, 15, 757. doi: 10.7150/ijbs.28461.
39. Allen, R.D.; Griffin, J.L. The time sequence of early events in the fertilization of sea urchin eggs. *Exp. Cell Res.* **1958**, 15, 163–173. doi:10.1016/0014-4827(58)90072-7.
40. Green, J.D.; Summers, R.G. Formation of the cortical concavity at fertilization in the sea urchin egg. *Dev. Growth Differ*. **1980**, 22, 821–829. doi: 10.1111/j.1440-169X.1980.00821.x.
41. Stack, C.; Lucero, A.J.; Shuster, C.B. Calcium-responsive contractility during fertilization in sea urchin eggs. *Dev. Dyn*. **2006**, 235, 1042–1052. doi:10.1002/dvdy.20695.
42. Mangini, M.; Limatola, N.; Ferrara, M.A.; Coppola, G. Chun, J.T.; De Luca, A.C.; Santella, L. Application of Raman spectroscopy to the evaluation of F-actin changes in sea urchin eggs at fertilization. *Zygote*, **2024**, 32, 38 – 48. doi.org/10.1017/S0967199423000552.
43. Steinhardt, R.A.; Mazia, D. Development of K^+-conductance and membrane potentials in unfertilized sea urchin eggs after exposure to NH_4OH. *Nature* **1973**, 241, 400–401. doi.org/10.1038/241400a0.
44. Winkler, M.M.; Grainger, J.L. Mechanism of action of NH_4Cl and other weak bases in the activation of sea urchin eggs. *Nature* **1978**, 273, 536–538. doi: 10.1038/273536a0.
45. Shen, S.S.; Steinhardt, R.A. Direct measurement of intracellular pH during metabolic derepression of the sea urchin egg. *Nature* **1978**, 272, 253–254. doi: 10.1038/272253a0.
46. Carron, C.P.; Longo, F.J. Relation of cytoplasmic alkalinization to microvillar elongation and microfilament formation in the sea urchin egg. *Dev. Biol.* **1982**, 89:128–137. doi: 10.1016/0012-1606(82)90301-3.
47. Begg, D.A.; Rebhun, L.I. pH regulates the polymerization of actin in the sea urchin egg cortex. *J. Cell Biol*. **1979,** 83, 241–248. doi: 10.1083/jcb.83.1.241.
48. Yonemura, S.; Mabuchi, I. Wave of Cortical Actin Polymerization in the Sea Urchin Egg. *Cell Motil. Cytoskel*. **1987**, 7: 46–53. doi: 10.1002/cm.970070107.
49. Longo, F.J.; Anderson, E. The effects of nicotine on fertilization in the sea urchin, *Arbacia punctulata*. *J. Cell Biol*. **1970**, 46, 308–325. doi:10.1083/jcb.46.2.308.
50. Tilney, L.G.; Jaffe, L.A. Actin, microvilli, and the fertilization cone of sea urchin eggs. *J. Cell Biol*. **1980**, 87, 771-82. doi: 10.1083/jcb.87.3.771.

 doi:10.20944/preprints202506.0164.v1

51. Limatola, N.; Vasilev, F.; Santella L.; Chun, J.T. Nicotine Induces Polyspermy in Sea Urchin Eggs through a Non-Cholinergic Pathway Modulating Actin Dynamics. *Cells* **2020**, 9, 63. doi.org/10.3390/cells9010063.
52. Sharon, N.; Lis, H. Lectins: cell-agglutinating and sugar-specific proteins. *Science* **1972**,177, 949-59. doi: 10.1126/science.177.4053.949.
53. Lallier, R. Effects of concanavalin on the development of sea urchin egg. *Exp. Cell Res*. **1972**, 72,157-163. doi.org/10.1016/0014-4827(72)90577-0.
54. Veron, M.; Shapiro, B.M. Binding of concanavalin A to the surface of sea urchin eggs and its alteration upon fertilization. *J. Biol. Chem.* **1977**, 252, 1286-92.
55. Veron, Mù.; Foerder, C.; Eddy, E.M.; Shapiro, B.M. Sequential biochemical and morphological events during assembly of the fertilization membrane of the sea urchin. *Cell* **1977**, 10, 321-328. doi.org/10.1016/0092-8674(77)90226-4.
56. Shapiro, B.M.; Eddy, E.M. When Sperm Meets Egg: Biochemical Mechanisms of Gamete Interaction. *Int. Rev. Cytol.* **1980**, 66, 257-30. doi.org/10.1016/S0074-7696(08)61976-2
57. Longo, F.J. Effects of concanavalin A on the fertilization of sea urchin eggs. *Dev. Biol*. **1981**, 82 197–202. doi:10.1016/0012-1606(81)90443-7.
58. Limatola, N.; Chun, J.T.; Santella, L. Fertilization and development of *Arbacia lixula* eggs are affected by osmolality conditions. *Biosystems* **2021**, 206, 104448. doi.org/10.1016/j.biosystems.2021.104448.
59. Vacquier VD (2012) The quest for the sea urchin egg receptor for sperm. Biochem Biophys Res Commun Aug 425:583-7 https://doi.org/10.1016/j.bbrc.2012.07.132
60. Lim, D; Lange, K.; Santella, L. Activation of oocytes by latrunculin A. *FASEB J.* **2002**, 16, 1050-6. doi: 10.1096/fj.02-0021com.
61. Terasaki, M. Visualization of exocytosis during sea urchin egg fertilization using confocal microscopy. *J. Cell Sci.* **1995**, 108, 2293–2300. doi: 10.1242/jcs.108.6.2293.
62. Limatola, N.; Chun, J.T.; Santella, L. Effects of Salinity and pH of Seawater on the Reproduction of the Sea Urchin *Paracentrotus lividus*. *Biol. Bull*. **2020**, 239, 13-23. https://doi.org/10.1086/710126.
63. García-Soto, J.; Darszon, A. High pH-induced acrosome reaction and Ca^{2+} uptake in sea urchin sperm suspended in Na^{+}-free seawater. *Dev. Biol.* **1985**, 110, 338–345. doi: 10.1016/0012-1606(85)90093-4.
64. Su, Y.H.; Chen, S.H.; Zhou, H.; Vacquier, V.D. Tandem mass spectrometry identifies proteins phosphorylated by cyclic AMP-dependent protein kinase when sea urchin sperm undergo the acrosome reaction. *Dev. Biol.* **2005**, 285, 116–125. doi.org/10.1016/j.ydbio.2005.06.007.
65. Schatten, G.; Mazia, D. The penetration of the spermatozoon through the sea urchin egg surface at fertilization. Observations from the outside on whole eggs and from the inside on isolated surfaces. *Exp. Cell Res.* **1976**, 98, 325-337. doi.org/10.1016/0014-4827(76)90444-4.
66. Epel, D. Mechanisms of Activation of Sperm and Egg During Fertilization of Sea Urchin Gametes. *Curr. Top. Dev. Biol*. **1978**, 12, 185–246. doi:10.1016/s0070-2153(08)60597-9.
67. Vacquier, V.D. The fertilizing capacity of sea urchin sperm rapidly decreases after induction of the acrosome reaction. Dev. Growth Differ. 1979, 21, 61–69. doi:10.1111/j.1440-169x.1979.00061.x.
68. Chun, J.T.; Vasilev, F.; Limatola, N.; Santella, L. Fertilization in Starfish and Sea Urchin: Roles of Actin. *Results Probl. Cell Differ*. **2018**, 65, 33–47. doi: 10.1007/978-3-319-92486-1_3.
69. Lopo, A.C.; Glabe, C.G.; Lennarz, W.J. Vacquier, V.D. Sperm-egg binding events during sea urchin fertilization. *Ann. NY Acad. Sci*. **1982**, 383, 405-425. doi: 10.1111/j.1749-6632.1982.tb23181.x.
70. Vacquier, V.D.; Swanson, W.J.; Hellberg, M.E. What have we learned about sea urchin bindin? *Develop. Growth Differ*. **1995**, 37, 1-10. doi: 10.1111/j.1749-6632.1982.tb23181.x.
71. Jaffe, L.A. Fast block to polyspermy in sea urchin eggs is electrically mediated. *Nature* **1976**, 261, 68-71. doi: 10.1038/261068a0.
72. Barresi M.J., Gilbert S.F. Developmental Biology. 13th ed. Oxford University Press; New York, NY, USA: 2024. Fertilization. Beginning a new organism; pp. 211–246. Chapter 7.
73. Schuel, H. The prevention of polyspermic fertilization in sea urchins. *Biol. Bull.* **1984**, 167, 271–309. doi:10.2307/1541277.
74. Wozniak, K.L.; Carlson, A.E. Ion channels and signaling pathways used in the fast polyspermy block. Mol. Reprod. Dev. 2019, 87, 350-357. doi.org/10.1002/mrd.23168.

 doi:10.20944/preprints202506.0164.v1

75. Just, E. E. The fertilization reaction in *Echinarachnius Parma*. *Biol. Bull.* **1919**, 36, 1–10.
76. Just, E.E. The Biology of the Cell Surface; P. Blakiston's Son & Co.: Philadelphia, PA, USA, 1939.
77. Dale, B.; De Santis, A. The effect of cytochalasin B and D on the fertilization of sea urchins. *Dev. Biol.* **1981,** 83, 232-237. https://doi.org/10.1016/0012-1606(81)90469-3.
78. Créton, R.; Jaffe, L.F. Role of calcium influx during the latent period in sea urchin fertilization. *Dev. Growth Differ*. **1995**, 37, 703-709. doi: 10.1046/j.1440-169X.1995.t01-5-00008.x.
79. Lange, K. Microvillar Ca++ signaling: A new view of an old problem. *J. Cell. Physiol*. **1999**, 180:19–34.
80. doi.org/10.1002/(SICI)1097-4652(199907)180:1<19::AID-JCP3>3.0.CO;2-K
81. Steinhardt, R.; Epel, Epel, D.; Carroll, E.J.Jr.; Yanagimachi, R. Is calcium ionophore a universal activator for unfertilised eggs? *Nature* **1974**, 252, 41–43. doi.org/10.1038/252041a0
82. Schmidt, T.; Patton, C.; Epel, D. Is there a role for the Ca^{2+} influx during fertilization of the sea urchin egg? *Dev. Biol*. **1982** 90, 284-90. doi: 10.1016/0012-1606(82)90377-3.
83. Stricker, S.A.; Centonze, V.E.; Paddock, S.W.; Schatten, G. Confocal microscopy of fertilization-induced calcium dynamics in sea urchin eggs. *Dev. Biol.* **1992,** 149, 370-80. doi: 10.1016/0012-1606(92)90292-o.
84. Galione, A.; McDougall, A.; Busa, W.B.; Willmott, N.; Gillot, I.; Whitaker, M. Redundant mechanisms of calcium-induced calcium release underlying calcium waves during fertilization of sea urchin eggs. *Science* **1993**, 261, 348-52. doi: 10.1126/science.8392748.
85. Whitaker, M.J.; Swann, K. Lighting the fuse at fertilization. *Development* **1993**, 117, 1-12. doi.org/10.1242/dev.117.1.1
86. Galione, A. Cyclic ADP-ribose, the ADP-ribosyl cyclase pathway and calcium signaling. *Mol. Cell Endocrinol.* **1994**, 98, 125-131. doi.org/10.1016/0303-7207(94)90130-9.
87. Carroll, D.J.; Albay, D.T.; Terasaki, M.; Jaffe, L.A.; Foltz, K.R. Identification of PLCgamma-dependent and -independent events during fertilization of sea urchin eggs. *Dev. Biol*. **1999,** 206, 232-47. doi: 10.1006/dbio.1998.9145.
88. Parrington, J.; Davis, L.C.; Galione, A.; Wessel, G. Flipping the switch: How a sperm activates the egg at fertilization. *Dev. Dyn*. **2007**, 236, 2027-2038. doi.org/10.1002/dvdy.21255.
89. Jiang, H.; Wen, X.; Zhang, X.; Zhang, B. Concanavalin A inhibits human liver cancer cell migration by regulating F-actin redistribution and assembly via MAPK signaling pathway. *Oncol. Lett*. **2022**, 24, 405. doi: 10.3892/ol.2022.13525.
90. Huldani, H.; Rashid, A.I.; Turaev, K.N.; Opulencia, M.G.C.; Abdelbasset, W.K.; Bokov, D.O.; Mustafa, Y.F.; Al-Gazally, M.E.; Hammid, A.T.; Kadhim, M.M.; Ahmadi, S.H. Concanavalin A as a promising lectin-based anti-cancer agent: the molecular mechanisms and therapeutic potential. *Cell Commun. Signal* **2022**, 20, 167. doi.org/10.1186/s12964-022-00972-7